Temperature Dependent Magnetic Response of $(Co_3O_4)_x$/CuTl-1223 Nanoparticles-Superconductor Composites

by

Mirza Hassan Baig
(420-FBAS/MSPHY/S16)

Supervisor

Dr. Muhammad Mumtaz

Associate Professor

Department of Physics, FBAS,

IIUI, Islamabad

Department of Physics

Faculty of Basic and Applied Sciences

International Islamic University, Islamabad

(2018)

Temperature Dependent Magnetic Response of $(Co_3O_4)_x$/CuTl-1223 Nanoparticles Superconductor Composites

by

Mirza Hassan Baig
(420-FBAS/MSPHY/S16)

This Thesis submitted to Department of Physics International Islamic University Islamabad, for the award of degree of
MS Physics.

CHAIRMAN
DEPT OF PHYSICS
International Islamic University

Chairman, Department of Physics Islamabad
International Islamic University, Islamabad

M . Axxl

Dean Faculty of Basic and Applied Science
International Islamic University, Islamabad

Department of Physics
Faculty of Basic and Applied Sciences
International Islamic University, Islamabad

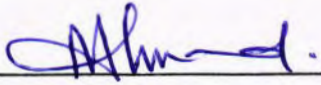**(2018)**

ii

Final Approval
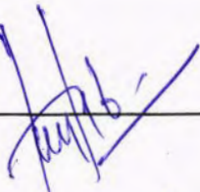
It is certified that the work printed in this thesis entitled **"Temperature Dependent Magnetic Response of $(Co_3O_4)_x$/CuTl-1223 Nanoparticles Superconductor Composites"** by **Mirza Hassan Baig**, registration No.420-FBAS/ MSPHY/ S16 is of sufficient standard in scope and quality for award of degree of MS Physics from Department of Physics, International Islamic University, Islamabad, Pakistan.
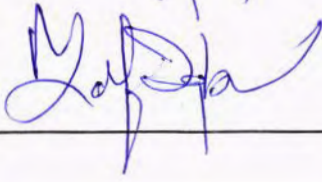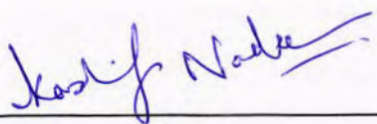
Viva Voce Committee

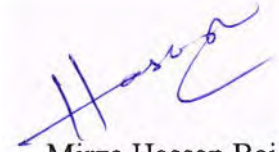Chairman (Physics)

Supervisor

External Examiner

Internal Examiner

DEDICATED

TO

MY BELOVED PARENTS

AND

RESPECTED TEACHERS.

Declaration

I, **Mirza Hassan Baig**, Reg No.420-FBAS/ MSPHY/ S16, student of MS Physics (2016-2018), here declare that the matter printed in the thesis titled "**Temperature Dependent Magnetic Response of $(Co_3O_4)_x$/CuTl-1223 Nanoparticles Superconductor Composites**" is my own work and has not been published or submitted as research work or thesis in any form in any other university or institute in Pakistan or aboard.

Mirza Hassan Baig
(420-FBAS/MSPH/S16)

Dated: 22/5/18

Forwarding Sheet by Research Supervisor

The thesis titled **"Temperature Dependent Magnetic Response of $(Co_3O_4)_x$/CuTl-1223 Nanoparticles-Superconductor Composites"** submitted by **Mirza Hassan Baig** (Reg. No. 420-FBAS/MSPHY/S-16) in partial fulfillment of MS degree in Physics has been completed under my guidance and supervision. I am satisfied with the quality of his research work and allow him to submit this thesis for further process to graduate with Master of Science degree from Department of Physics, as per International Islamic University Islamabad, Pakistan, rules and regulations.

Dr. Muhammad Mumtaz
Associate Professor (TTS)
Department of Physics,
International Islamic University,
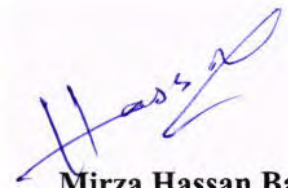Islamabad.

Dated: 23/05/18

Acknowledgement

I have no words to express my deepest sense of gratitude and numerous thanks to **Almighty Allah**, who enabled me to complete this study and with innumerable blessings for the **Holy Prophet Peace Be upon Him** who is forever a torch of guidance and knowledge for the whole humanity.

I would like to thank my supervisor **Dr. Muhammad Mumtaz**. Firstly, for taking me on as a student and then for providing support, advice for letting me develop my own ideas, and for helping me make it to the end. I would like to pay lots of appreciation to all my teachers.

My journey wouldn't have been the same without the lab fellows for all the conversations that we had over the year, they always made me smile when the lab days just weren't going right. I appreciate the services of all my senior research colleagues, **Abrar Ahmad Khan, Hassan Shabbir, M. Qasim , Ali Usman** and especially **Liaqat Ali** for being very supportive and co-operative all throughout my research work. I also pay special thanks to **Dr.Waqi** for being helpful in all my research work.

My humble and heartfelt gratitude is reserved for my beloved Parents. Without their prayers and encouragement, the completion of this task would have been a dream. I am extremely thankful to my friends.

May Allah bless all these people.

Mirza Hassan Baig

Contents

Abstract

Solid-state reaction method was used to synthesize $Cu_{0.5}Tl_{0.5}Ba_2Ca_2Cu_3O_{10-\delta}$ (CuTl-1223) superconducting phase and sol-gel method was used to prepare cobalt oxide (Co_3O_4) magnetic nanoparticles. These Co_3O_4 nanoparticles were added in CuTl-1223 superconducting matrix to get $(Co_3O_4)_x$/CuTl-1223; x = 0 ~ 2.00 wt.% nanoparticles-superconductor composites. The effects of Co_3O_4 nanoparticles on crystal structure, phase formation, phase purity and infield superconducting transport properties of CuTl-1223 phase were investigated at different operating temperatures and external applied magnetic fields. The crystal structure and phase formation of Co_3O_4 nanoparticles and CuTl-1223 superconductor were determined by X-ray diffraction (XRD) technique. XRD peaks of Co_3O_4 nanoparticles were well indexed according to FCC crystal structure and the average particle size of 70 nm was calculated by using Debye-Scherer's formula. The unaltered crystal structure of host CuTl-1223 superconducting phase (i.e. Tetragonal) with the addition of Co_3O_4 nanoparticles indicated the dispersion of nanoparticles at inter-granular sites. Temperature dependent magneto-transport superconducting properties of $(Co_3O_4)_x$/CuTl-1223 composites were investigated by zero field cooled (ZFC) and field cooled (FC) magnetic moment versus temperature (M-T) measurements. The onset transition temperatures $\{T_c^{Onset} (K)\}$ was decreased along with the suppression of diamagnetic amplitude of CuTl-1223 superconducting phase with the addition of magnetic Co_3O_4 nanoparticles. Temperature dependent magnetic hysteresis (M-H loops) measurements of $(Co_3O_4)_x$/CuTl-1223 composites were carried out at different operating temperatures from 5 K to 150 K. Critical current density (J_c) was calculated from M-H loops measurements by using Bean's model. Like the suppression of T_c^{Onset} (K) values, J_c was also decreased with the inclusion of Co_3O_4 nanoparticles. It was also observed that variation of J_c with H followed the power law $J_c = \beta H^{-\alpha}$ at low operating temperatures 5 K and 20 K only.

Chapter No.1

Introduction

1.1 Superconductor

Most of the materials such as metals and alloys exhibit the resistivity almost zero after cooling at sufficiently low temperatures and they also repel the applied external magnetic field thus such type of metals and alloys are called superconductor materials. [1] The first superconductor was discovered by Kimberling Onnes in 1911.He observed that at low temperature material show almost zero resistance and conductivity becomes maximum [2,3]. In 1933 W. Meissner and R. Ochsenfeld observed the second characteristic of superconductor that applied external magnetic field continuously expelled by material at low temperature. This, phenomena of expulsion of external magnetic field is called Meissner effect. Basically, Meissner effect reveals the diamagnetic behavior of the superconductors [4].
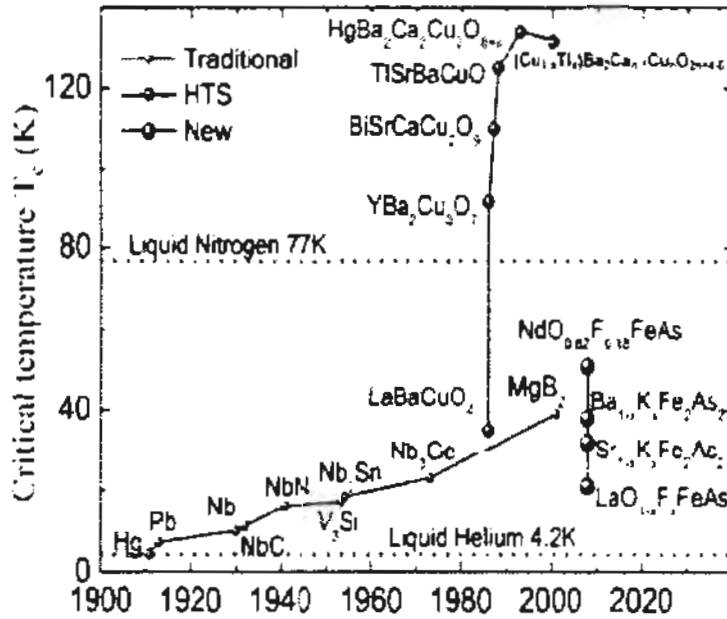
Fig 1.1: Historical development of superconductor families[1].

In 1957 John Bardreen, Leon Cooper and J. Robert proposed BCS theory to explain the phenomena of superconductivity using the concept of cooper pair. Cooper pair formation occurs when electron above the fermi level attract to other electron rather than repulsion due to phonons which is produced due to lattice vibration. BCS theory gives theoretical description for

superconductivity in superconductors by formation of cooper pair [5,6]. In 1986 Bednorz and Muller discovered a new class of superconductors which is known as the high temperature superconductors (HTSCs) [7]. Now a day's composites of high temperature superconductors are under study for maintenance of high critical current density at high temperatures. The phenomena of superconductivity depend on three major parameters which are given as follow.

1. Critical Temperature
2. Critical magnetic field
3. Critical current density

1.1.1 Critical temperature

The temperature at which material remains in superconducting state and above this temperature superconductivity in material destroyed is called critical temperature. It is denoted by T_c. It is also known as the transition temperature of material. Until now purpose of discovery of superconductors is to achieve or reach transition temperature at room temperature [8].

1.1.2 Critical magnetic field

When a superconductor material face to applied external magnetic field then it expels it up to specific value after that magnetic field start penetrating in to material and destroy the superconductivity. Thus value of magnetic field in which superconducting material changes from superconducting to normal material is called critical magnetic field. It is denoted by H_c [9].
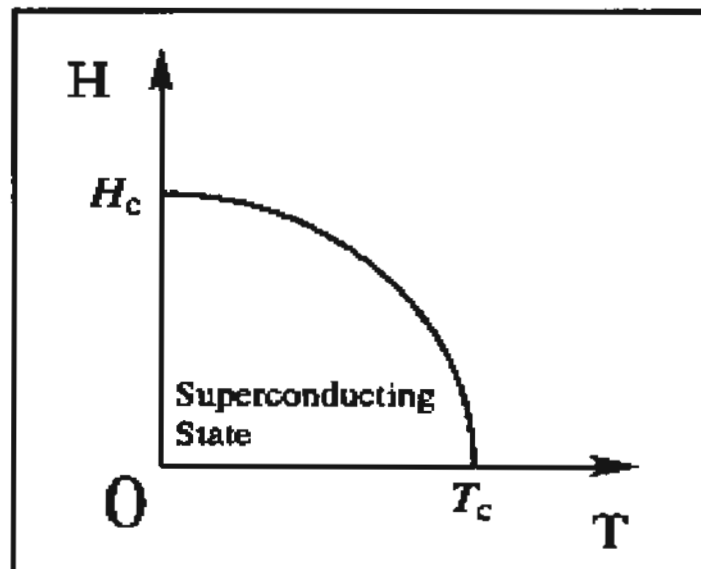
Fig 1.2 Graphical relation between H_c and T [2]$_c$

The relationship between H_c and T_c given as follow:

$$H_c = Ho \ [1-(T/T_c)^2] \ \ldots\ldots 1.1$$

1.1.3 Critical current density

The superconducting material transfer maximum current without offering any resistance or without changing in to the normal material is called critical current density. It is denoted by J_c. The superconducting material below Jc remains superconductor but above Jc it becomes normal material [10].
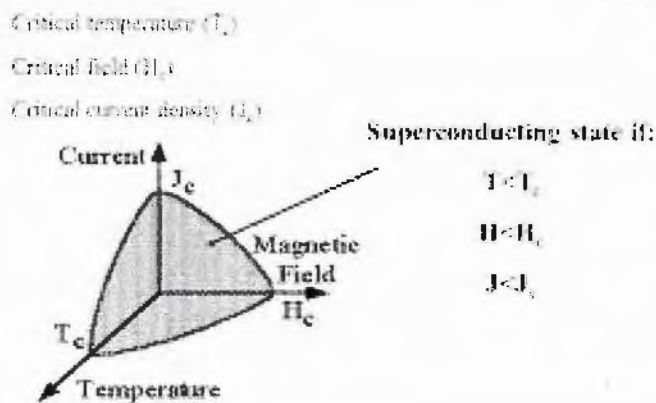
Fig1.3: Relationship between H_c J_c and T_c[3]

Given above figure shows the relationship graphically between the three critical parameters of the superconductivity phenomena which also shows the limits of superconductor material for remaining in the superconducting state and how they depend on these given critical parameters.

1.2 Meissner effect

In 1933, there were two scientists named as W. Meissner and R. Ochsenfeld who discovered that a material which is in superconducting state placed in an external magnetic field completely expelled the applied external field then effect of this superconductor called Meissner effect. The expulsion of applied external fields proves a diamagnetic property of superconductor. This property of superconductor depends on the value of the applied external field, whenever the value of applied external magnetic field exceeds the critical value (H_c) the superconducting property vanishes in the given material [11].In fig 1.4 Meissner effect is shown
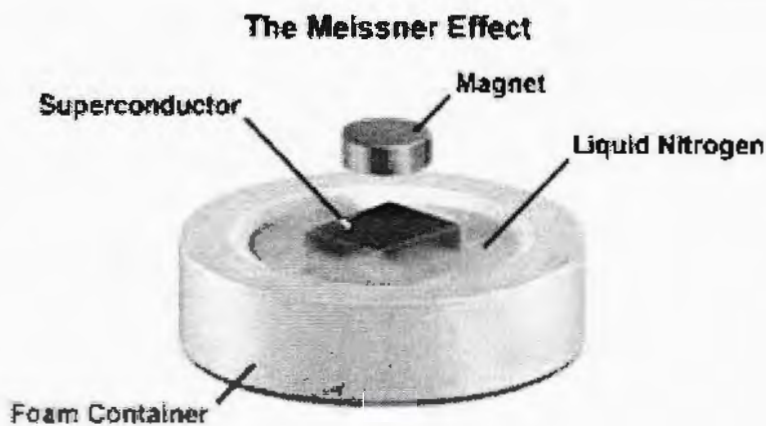
Fig 1.4: Meissner effect [4]

1.3 Classification of Superconductors

Meissner effect, basically classifies the superconductors in two types due to expulsion of magnetic field up to different levels [12].

1.3.1 Type-I superconductors

Type -I are those superconductors which abruptly lose the superconducting state when the external magnetic field is across the critical value of Hc Due to an abrupt loss of superconducting properties type -I called soft super conductors. Type-I superconductors also exhibit the complete Meissner effect. There is no mixed state in type-I superconductors. Below Hc they remain in the superconducting state and above Hc they transform into the normal material. Tin and mercury are pure metals which have a low value of H_c thus they are known as type-I superconductors. Type-I superconductors have H_c value material dependent because different materials have a different value for the expulsion of externally applied magnetic field. Examples of type-I superconductors are Zn, Al, Sn and Hg [13].

1.3.2 Type-II superconductors

The superconducting materials which lose the superconductivity steadily are called as type-II superconductors. This class of superconductors also known as hard superconductors because they lose superconductivity in steady form in contradiction to type-I superconductor in which material loses superconductivity abruptly. Type-II superconductors as lose their superconductivity gradually in three different states, which are named as follow.

1. Meissner or superconducting
2. Vortex

3. Normal

Due to these states which exist in type-II superconductors, they consist of two critical magnetic fields Hc1 and Hc2.where as Hc1 is a lower critical field and Hc2 is an upper critical field. These two fields specify the current state of superconductors. If field applied to the material below Hc1 then they exist in state of Meissner or superconducting. If field applied to material between Hc1 and Hc2 then they exist in vortex state. If the field given to material is greater than Hc2 then material completely changes into normal state. Thus type-II superconductors not completely exist the Meissner effect. Examples of type-II superconductors are Zr and Nb [14].
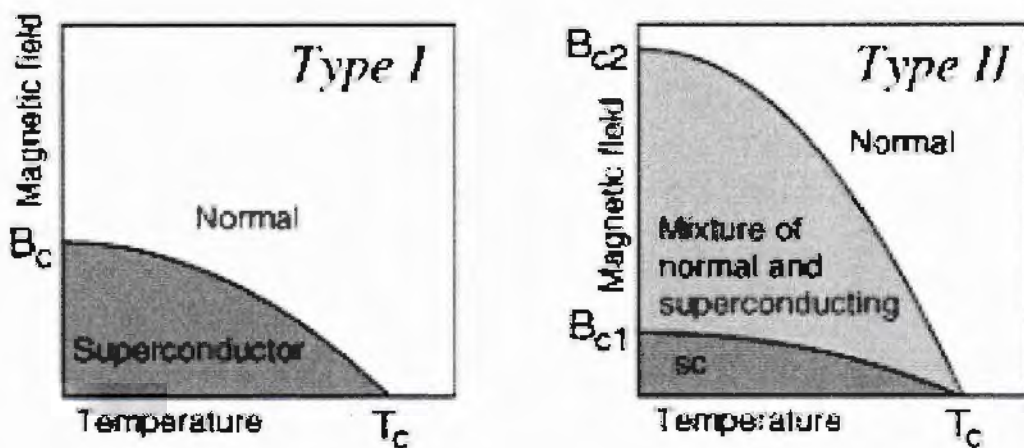
Fig 1.5: Graphical representation of Type-I and Type-II Superconductors[6].

1.4 High Temperature Superconductors

K. Muller and J. Bednorz discovered the first high temperature superconductor in 1986 and both wrer awarded with noble prize for their discovery. High temperature superconductors mean superconductors which contain high critical temperature almost above the 35k.The purpose of new class of superconductors to achieve the room temperature superconducting materials. High temperature superconductor interchangeably with cuprate superconductors such as yttrium barium copper oxide (YBCO) and bismuth strontium calcium copper oxide (BSCCO). In 2008, Iron based superconductors were discovered. BCS theory tells us about the formation of cooper pair and coherence length. The coherence length of cooper pair contrast with interatomic distance is larger usually in low temperature superconductors. Coherence length depends upon the anisotropy of the material. In high temperature superconductors the coherence length is equal to 1-2 nm. High temperature superconductors have coherence length low as compared to low temperature superconductors [15].

1.4.1 Zero Resistivity

In superconducting materials, below a certain temperature conductivity becomes infinite whereas resistivity becomes extremely low almost equal to zero. The condition of zero resistivity exists in material when there is a flow of persistent current in it. Then current only due to the flow of conduction electrons in superconducting material. Thus, certain temperature is known as critical temperature. According to critical temperature a material can be characterized in two states. One is normal and other is superconducting state. Above the critical temperature materials in state of normal. On the other hand, below the critical temperature material should be superconducting state. In superconducting materials, critical current density has some definite value and electric field always be zero. Thus, current flow in superconducting material in the absence of electric field. The properties of normal state and superconducting state materials are totally different. Graphical representation of superconducting and normal state materials is given below in figure.
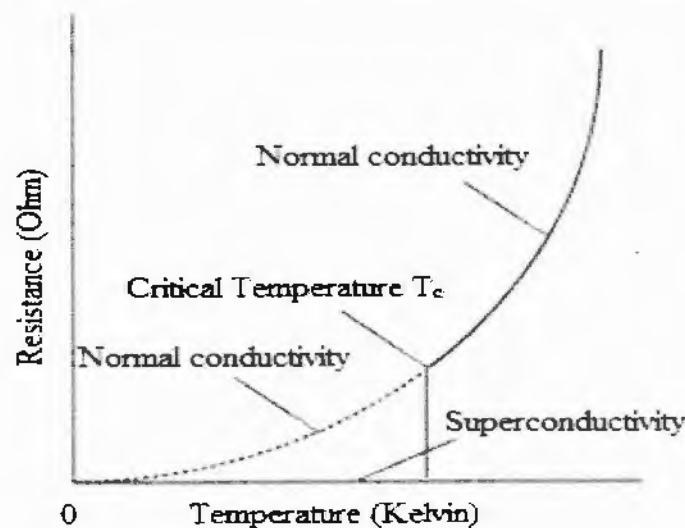
Figure 1.5: Graphical representation of normal and superconducting state of material[6]
Resistivity value of a material directly effects the properties of material such as the chemical and physical properties of a material. Thus number of materials which have its own value of resistivity on the basis of resistivity value material used for different type of applications.

1.5 Nomenclature

According to IUPAC, nomenclature of high temperature superconductors (HTSCs) consists on two parts. The first part of HTSC explains the name of composites which are written in capital letter. Such as Y-Ba-Cu-O written as YBCO. Where is another superconductor composites written as BSCCO (Bi-Sr-Ca-Cu-O). The stoichiometry of compound given by second

part of the HTSC. Example are as Y123 contain stoichiometry $YBa_2Cu_3O_{7-x}$ where as Nd422 written as $Nd_4Ba_2Cu_2O_{10-x}$ [16].

1.6 Cuprates

The cuprates compounds lay on two series such as BSCCO and TBCCO show the transition from 60 k to 125 k. Peculiar structure of these compounds are orthorhombic and tetragonal in nature. Two layers in compound structure are responsible for superconductivity phenomena [17].

1- Charge reservoir layer

2- Superconducting layer

Unit cell of these compounds contains two-layer structures. One layer which is CuO2 plane is superconducting plane. Whereas layer depends on remaining of atoms which form the charge reservoir layer. Atoms in charge reservoir are Tl, Hg, Bi, Cu, and Ba. These layers are separated by Calcium atoms. The supplier of charges to CuO2 layer is charge reservoir layer. Cooper pair formation occurs, when charges move from charge reservoir layer to superconducting layer. The superconductivity of material demonstrated by the coherence length of the cooper pair and its formation. The number of charge carrier present in the reservoir layer gives us information about the critical or transition temperature of superconducting material [18,19]. The transition temperature of the superconductor also influenced by a number of charge reservoirs. In superconductor CuTl-1223 vary the amount of thallium oxide then transition temperature also increases. If we increase superconducting plane in our material such as copper oxide, then decreases in T_c occur [20].
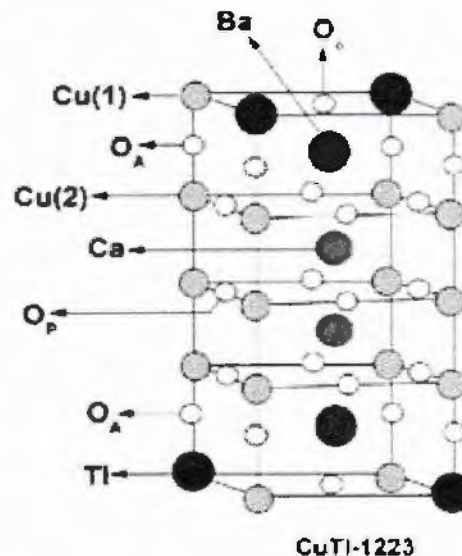
CuTl-1223

Fig 1.6. Unit cell of CuTl-1223 superconductor [7].

1.7 BCS Theory

The origin of superconductivity determined by the BCS theory. This theory, in 1957 is projected by three scientists, Bardeen, Cooper and Schrieffer. BCS theory gives the idea of cooper pair formation due to phonons which are produced by lattice vibration. This theory explains that when an electron passing through positive charge clouds it produce a disturbance in the lattice. Due to lattice vibration phonons are emitted and these phonons dominate the repulsive force between two electrons
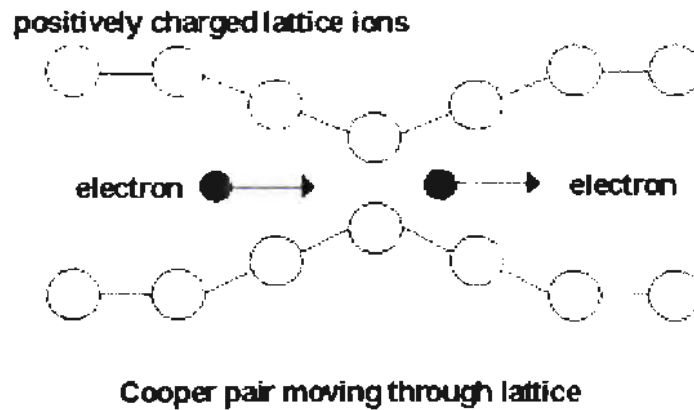
Fig 1.7. Formation process of Cooper pairs [8]

.   Thus, at particular distance two electrons form a pair due to these phonons. In this way, the formation of a pair of electrons is known as cooper pair. BCS theory is a theoretical approach to reveals the concept of superconductivity in a superconducting material. Cooper pair formation is basically occurrence of Bosons. When half integral spin containing electrons, both combine form a spin zero boson at ground level. Thus, superconductivity phenomena are theoretically explained by the BSC theory [22].

1.8 Nanomaterials

Commonly nano size material is defined as a material having a size less than 1nm or those materials which cannot he seen by a normal human eye. We say in science language, these materials are nano-materials. The properties of nano materials are totally different from normal materials. Nanomaterials have different structures due to confinement of electrons in all directions. Due to the arrangement of electrons in all directions, nanomaterials are classified such as zero dimensional, one dimensional and two dimensional. whereas an example of zero-D is Quantum dot, one-D is nanowires and two-D is nano thin films. The nanomaterials played a vital role in the life of human being. Nanomaterials applications in a lot of numbers because they used in a number of which things are used in daily life or in rare cases. In each field of life, nanomaterials become

important to human being. This is all due to its peculiar specifications for example its volume to surface ratio increase then its properties increase which is in case of bulk materials. The Characteristics of nanomaterials changed the from bulk to nano scale. In daily use equipment nanomaterials show extraordinary changing in it. Such as light weight of cars bikes and computer chips. Where as in the field of medical and Health, nanomaterials are used to diagnosis the disease earlier. Nanomaterials also used for the treatment of cancers. Gold nanomaterials also used as a key point for detection of nucleic acid [23]. Classification of nanomaterials based on confinement of electrons in these materials. Thus, nanomaterials classified in to zero, one, two and three dimensional.

1.8.1 Zero dimensional materials

The confinement of electrons in three directions in a material is known as zero dimensional materials. The size range of zero-dimension materials vary from one nanometer to ten nanometers. Dimension of the materials is smaller than that of the thermal wavelength of the fermi electrons. Examples are quantum dot and nanoparticles. The structures of these materials may be crystalline and amorphous [24].

1.8.2 One dimensional materials

Those type of materials in which movement of electrons allowed in one direction and confined in two directions known as one dimensional material. Examples of these materials are nanotubes, nano wires and nano rods. Thus, the structure of these materials exists in form of crystalline, amorphous and polycrystalline. The most common material used as one dimensional are metallic, ceramic and polymeric [25].

1.8.3 Two dimensional materials

Those materials which allowed the movement of electrons in two dimensions and restrict in one dimension are called two dimensional nano- materials. The range of two dimensions in micro level while in the one-dimension range is nanometer. Common examples are nanolayers, nanofilms and quantum well. The structure of these materials in the form of amorphous and crystalline. These materials may be pure or impure because they consist of different composition [26].

1.8.4 Three dimensional materials

Those materials in which electrons move freely in any direction of a materials and are not restricted and the size of these materials larger than 100 nm.

1.9 Magnetic materials

All kind of materials have magnetic properties which are classified due to their response on the applied external field. In periodic table. highlight the magnetic elements and they are arranged in it. Magnetism generalized form explained by diamagnetic material also with para-magnetic materials because both materials are present in a lot of numbers in the periodic table.

Fig 1.8. Classification of materials in the periodic table[9]

1.9.1 Paramagnetic materials

When a magnetic material is placed in external applied magnetic field and its domain aligned in direction of an applied field until the field is present and their domain become in disorder state when the field is removed. Such type of materials shows positive magnetization under the presence of applied magnetic field. Whenever the temperature is increased, then there is hard to align the magnetic moments in direction of field because of the thermal energy increased due to this effect there is decrease in susceptibility. Such type of phenomena is explained by curie law.

Pauli model obeys those materials in which free electrons exist and collide to form a conduction band. Pauli model explains that in presence of applied field an imbalance set up between free electrons with opposite spin. Then the result is that low magnetization, occur in response to applied field [27].

1.9.2 Diamagnetic materials

When a material is placed in the applied external magnetic field, it does not respond to applied external field or their domains aligned opposite to the applied magnetic field thus such

type of materials classified as diamagnetic materials. These materials show negative magnetization under the applied external magnetic field [28].

1.9.3 Ferromagnetic materials

When a material is placed in applied external magnetic field, they response to the applied external field or their domains aligned to the direction of the applied magnetic field. Remains aligned after removing applied field thus such type of materials are classified as ferromagnetic materials. These materials show positive magnetization always either field is applied or not to a material [29]

1.9.4 Antiferromagnetic materials

When a material is placed in the field then their magnetic moments aligned such that net magnetization is zero because they aligned opposite to neighbor. Thus, such type of materials is known as antiferromagnetic materials. Some materials are Manganese oxide, iron oxide, cobalt oxide, nickel oxide, chromium [30].

1.9.5 Ferrimagnetic materials

When a magnetic material is placed under applied magnetic field then they give the small value of magnetization because magnetic moments aligned opposite to each other and their values are not equal. Such type of magnetic materials known as ferri magnetic materials [30].

1.10 Nanotechnology and Nanoscience

The word "nano" taken from the Greek language which means very small. A minute or tiny but when we discuss Nano in nanotechnology. It means that we deal with one billionth part of a meter. Whereas the size of atom approximately equal to 10^{-15} meter while one nanometer is equal to 10-9 meter. Now we define as the study of materials at nanoscale is known as Nanoscience and fabrication of these nanomaterials is known Nanotechnology. The nanoscience exists in nature, before study of scientists in this field of science. All living things consist of building blocks which are in range of nanometers. In an inch, twenty-five lacks forty thousand nanometers exist. The thickness of newspaper sheet is almost about 1 lack. when there was scanning electron, microscope developed then age of the Nanotechnology started. Now a day scientist try to fabricate different types of materials at nanoscale so that they get more advantages [30].

1.10.1 Hysteresis loop

The loop which gives us information about magnetic properties of magnetic materials is known as a hysteresis loop. It gives us the relation between the applied field (H) and induced

magnetic field (M) of a material, which is called M-H loop of a magnetic material. Hysteresis loop is produced when we measured induced magnetic flux density of a material by changing applied field. Hysteresis loop basically tells us about losses of a material. When we study loop of a magnetic material then it gives us number of key magnetic properties of a material.

1.10.2 Retentivity

It is a measurement of residual flux density which is corresponded to induction of saturation of magnetic material. In other sense, the ability of a material to retrace the rest of magnetic flux when we removed force from the material after reached saturation.

1.10.3 Residual magnetic flux

The magnetic flux which is remained in the material after removing the magnetic field. when material reached the point of saturation then retentivity and rest of flux density will be same. Level of magnetic flux lesser than that of retentivity when we did not reach saturation.

1.10.4 coercive force

The force which is required to make residual flux equal to zero is known as coercive force or reverse magnetization.

1.10.5 Permeability

It is material property which clarifies that ease through which magnetic flux reputable in components.

1.10.6 Reluctance

When a magnetic material show opposition to the existence of magnetic field [31].

1.12 Bean Model

In 1962, C.P Bean gives an idea about irreversible magnetization of hard Superconductors by explaining its hysteresis. Hard superconductor shows hysteresis on calculations of its magnetization. Bean model postulated that shubnikov phase is a strange process only because of the existence of microstructure of materials. He supposed that lossless transport containing Jc is equal to constant or zero. In Meissner state externally, applied field is sheltered as in type-1 superconductors. where as in case of vortex state, critical current flow in depth of the surface of materials because to reduce the field inside of superconductors. According to Bean model evaluation of critical current density from M-H loops can be done by this following equation.

$$J_c = 20 \times \Delta M/D \dots\dots\dots\dots\dots\dots\dots\dots(1.1)$$

Where ΔM = M(increasing) – M(decreasing)

And   D is thickness of the sample

D=a(1-a/3b) while a<b and a,b are dimensions of sample.

ΔM means that value of positive magnetization and value of negative magnetization. Where D is the thickness of a material which depends on dimensions of a material [32].

1.12.1 Irreversible magnetization

For its understanding, we assume that applied magnetic field to hallow cylinder parallel to its axis when a votex state occurs in a type-II superconductor. Then vortices start to penetrate into the type-II superconductors. On its surface vortices are pinned. The area of surface up to which penetrate vortices is the critical current density (i.e.). The vortices do not approach the inner surface of the cylinder at the low applied field. Thus, there is no field inside the surface of the cylinder. When increased the value of field further there are vortices starts to penetrate in to the interior surface. Then decreased the value of the applied field, what happened to it. because of the induction at outer surface opposed critical current which keeps the constant current inside the surface of the hollow cylinder. When we remove the applied field then remnant field produced inside the surface of the cylinder. Thus, with an opposed external field there is a field inside the cylinder becomes zero [33].

1.12.2 Pinning in High Temperature Superconductors (HTS)

In high temperature superconductor (HTS), pinning of magnetic vortices brings mostly challenges for scientists which are working in the superconducting field. The movement of magnetic vortices in high temperature superconductors cause the loss of energy and the state of zero resistivity remains unstable (superconducting state). Grain boundaries, crystal defects and impurities are the common sources of natural pinning centers specially in the case of high temperature superconductors. Beside of these natural pinning centers, there may create some artificial pinning center by using some various techniques such as ion irradiation, different nanostructure addition and chemical doping. The pinning phenomena get disturbance by movement of magnetic vortices in superconductors. As result of magnetic vortices that flux starts to flow in high temperature superconductors. The motion of magnetic vortices categories into their different form depending upon the value of operating temperature and current density applied.

1- Thermally activated flux flow (TAFF)

This type of flux flows only possible when the value of current density is less than the critical current density in the magnetic vortices of high temperature superconductors.

2- Flux Creep (FC)

Such type of flux flows possible in magnetic vortices when the value of current density is equal than the critical current density in the high temperature superconductors.

3- Free flux flow (FFF)

Free flux flow defined as magnetic vortices shows the movement in such a way that value of current density is greater than the value of critical current density.

The value of current density also depends upon the operating temperature. Thus the change in operating temperature also effect the current density of high temperature superconductorss

1.12.3 Vortex in High Temperature Superconductors (HTS)

In a type-II superconductor, class of high temperature superconductor exists, because these types of superconductors have short coherence length ξ and long penetration depth λ that's why they have large Ginzburg landau parameter κ. A large value of κ has a direct effect then its results that H-T phase diagram contains the more of the area of the mixed state. Such type of effects is clear when seeking the expression of the upper and lower critical field. Penetration of the magnetic flux start in superconducting material when Gibbs free energy vortex exceeds from Gibbs free energy of the Meissner state. Just above the lower critical field penetration of vortex will start.

$$H_{c1} = \frac{\phi}{4\pi\mu\lambda^2} \ln \frac{\lambda}{\xi} \dots\dots\dots\dots\dots\dots\dots 1.2$$

Basically, in HTS contain a small region of Meissner state. Because of the low value of H_{c1}, which is governed by the long coherence length. On the other side, in H_{c2} means in upper critical field region vortices are high and the cores of these vortices start to overlap. The H_{c2} calculated by using the equation of the Ginzburg-Landau Theory.

$$H_{c2} = \frac{\phi}{2\pi\mu\xi^2} \dots\dots\dots\dots\dots\dots\dots\dots 1.3$$

In superconducting material value of short coherence length gives us the high value of the H_{c2}. Vortex state covers the large region in the Phase diagram of the HTS.

Vortices in the pure sample arranged through manner and repulsive force created by the super current, which kept the vortices apart from each other by repulsive force and which help to push out from the material. In presences of the vortices, energy is low whenever the field is above from

Hc1. The repulsive force created to prevent the vortices, from leaving the sample by taking the flux density constant. when forces established into equilibrium condition then vortices remained into arranged form.

The lattice of a vortex is named as Abrikosov vortex, because in 1957, Abrikosov gives solution by using linearized Ginzburg landau equation. Which prophesied that parallel flux lines are a lattice [34]. In 1967, concept of Abrikosov lattice taken by Essemann and Truble in the usage of bitter decoration on Pb-4 [35]. Further Gammel to observe the lattice by use of the same method, after the discovery of the yttrium-based superconductor (YBCO) [36]. After further developments, a number of techniques such as magnetic force microscope and tunneling microscope used for observing the vortices image [37]. Magneto optics and Lorentz microscopy techniques have been used for observations of dynamics of vortices [38].

1.12.4 Vortex Dynamics

When the current density is given to a superconductor in the case of mixed state then its response to a Lorentz force will create due to which motion of the vortices initiates in superconductor. When the motion of vortex start then forces per unit length of the vortex is.

$$f_L = j \times \phi \dots \dots \dots \dots \dots \dots \dots \dots \dots \dots \dots 1.4$$

whereas $\phi = \phi_0 \hat{z}$, considering that vortex is parallel to z-axis. Then Lorentz force over the entire sample of per unit volume as of equation 1.4. Thus magnetic flux is represented by the B. The flow of vortex is opposed by the viscous of the drag force as a result constant velocity gain by the vortices. Then vortex contain viscous drag force per unit length is

$$f_\eta = \eta \, v \dots \dots \dots \dots \dots \dots \dots \dots \dots \dots 1.5$$

In the above mention equation η represents the drag viscous coefficient. The motion of vortex is start due to the supply of electric field $E = v \times B$ and which is parallel to current density j.

Due to motion of vortex, power dissipation start as result of which perfect conductivity is disappeared.

For the recovery of perfect conductivity, there is another force required compulsory for the restriction or to stop the vortex motion, even in the presence of Lorentz force F_L. In the system of the real materials, presence of the static disorder results to a extra force in system. If in a material there are some defects then there is more chance for a vortex to be located in it, as a result depression in the order parameter occurred. However, randomly dispersion of pinning centers will not be effective to localize the vortex lattice. Since the sum of sperate pinning force from each

pinning site results add up to zero. In 1979, this problem is studied by the Larkin and Ovchinnikov in theory of pinning collectively [39].

The characteristic of dissipation of the free current flow is well again when disorder property is used to pinning the vortices. On the other side, when current density (j) becomes maximum than critical current density (j_c) of superconductor then Lorentz force overcome the pinning force due to which vortices start to move again. Critical current density bounded by the current due to which cooper pair can be destroyed. Which is known as despairing current density j_0, So $j_0 < j_c$. At low temperature pinning phenomena are more effective where thermal fluctuations are no more important. In another case where the temperature is high, then de-pairing rate becomes more than pairing rate even in the current density less than the critical current density.

Chapter no.2

Literature Review

G. Kirat and O. Kizilaslan, explain the results of structural, critical current density and magnetic properties in BSCCO glass ceramic superconductor with variation of nanoparticles in sample (x = 0, 0.5 and 1.0). The superconducting material was prepared by glass ceramic technique. The XRD diffraction gives us information about the material phase formation. The SEM was used for the morphology of superconducting materials. EDX analysis which reveals that Eibirm nanoparticles cover the interstitial sites of the material. The occupation of nanoparticles to interstitial sites gives us change in parameters of unit cell because of the smaller radius of copper ion as compared to Er ion. A significant effect of Er nanoparticles on the critical current density and magnetic properties of the materials. Because of the nanoparticles effect, material change in to paramagnetic from superconducting behavior. In the presence of magnetic field, substitution of Er in Cu ion sites results the enhancement of J_c and depressed in Tc at low level. When Er ions substituted in material with x= 0.5 there was obtained highest value of crtical current density at $1.25*10^5$ A cm^{-2} at 10 k. But further increase in value of nanoparticles was occurred to decrease in J_c. Thus, suitable increment value of critical current density occurs at x = 0.5 % [40].

H. P Kunkel and P. A. Stampe studied the temperature and field dependence of magnetization and also resistivity. They measured the AC susceptibility at various frequency of YNi_2B_2C. These data of yittrim based superconductor was provided by X ray measurement. Data about the field and temperature dependence of magnetization with transport properties of YNi_2B_2C was produced on sample by chill casting technique. Which results to enhancement of lower field, upper field and irreversible magnetization. The main effect of increase in J_c while slightly depressed T_c. All these effects   may be due to defects in a material which take place during manufacturing process. In high Tc cuprate superconducting materials, preliminary data reveals that there is reduction in parameters which is unannealed chill caste sample but these type results unexpected, which is indicating that defects might combined in some preferential alignments [41].

Aima Ramli and Hussein baqiah reported the effect of Nd_2O_3 nanoparticles on AC susceptibility, transport and microstructural properties of the $YBa_2Cu_3O_{7-\&}$ (Y123) ceramic superconductors. The $YBa_2Cu_3O_{7-\&}$ (Y123) superconductor material was manufactured successfully by co-precipitation method. Phase formation of $YBa_2Cu_3O_{7-\&}$ (Y123) superconductor material confirmed by XRD data analysis. Which confirm the perovskite structure of Y123 superconducting material and secondary phase of Y211 with x> 0.2 wt %. whereas SEM gives information that material has highest bulk density and the grains are linked as there is no pores exit between them. For x= 0.2 wt% structure of materials exists in form of porous and their grain size decreased. The addition of Nd_2O_3 in superconductor material, create the vacancy of oxygen disorder that results in reduction in transition temperature of material from 92K to 78k with x = 0 to x = 1.0%. when AC susceptibility measured by varying field from 0.005(oe) to 3 (oe) with Nd2O3 (x=0.0 to x=1.0) then there is broadening and wider intergranular peaks occur. which results the faintness of grain coupling? when x=0.6% of nanoparticles at field of 0.005(oe) then material attain the intergranular Jc with optimum value of $5.77*10^5$ A/cm^2. which shows that Nd_2O_3 nanoparticles acting as pinning center in $YBa_2Cu_3O_{7-\delta}$ (Y123) superconducting materials [42].

Shankar D. Birajdar and A.B Shinde studied the effect of iron doping in BaZrO3 nano-ceramic. Which is prepared by sol gel method having simple perovskite cubic structure. There is change in structure occur when iron atom is doped in BaZrO3 because values of lattice parameters, grain size, unit cell volume and crystallite size are changed. When iron atom doped in material then there is linearly reduction in lattice parameter (a) observed which is obeying the Vegard s law. FESEM show that particles are combined in such a way to form spherical shape with nanometer range. XRD data was supported by TEM results which explain the roughly size of nanoparticles. EDX result reveals that sample near to stoichiometry. The absorption band obtained from FTIR in range of 563 cm-1 to 596 cm-1 describing the cubic perovskite structure of sample. Increase concentration of Fe in results of this there is decrease of bond length of the (Fe/Ti—O). Induction of trivalent iron ions to tetravalent Zr sites produced the defects band which narrow the energy band gap due to difference of ionic radii and valance shell. Fe concentration increased as result of this magnetic order also increased. Below 50 k there is rapidly increased in magnetization which shows the temperature magnetization. At low temperature ferromagnetic behavior observed when

there was splitting in ZF and ZFC. The band gap becomes narrow with increased Fe concentration [43].

M. Hafiz and R. Abd-Shukor investigated the effect of the antiferromagnetic nanoparticles on structural and critical current density of the Bismuth based superconductor. NiF_2 tapes added to material which results in increased J_c as compared to nonadded tapes. The enhancement of J_c shows that nanoparticles behave as pinning centers for materials. The value of J_c becomes higher when material sintered at 100 h as compared to 50 h sintered sample because of improvement in inter grain connectivity. Thus, if sample was sintered to beyond 100 h then may be J_c further increased. Below 60 k their steeper increase in Jc very close to Neel temperature of NiF_2 nanoparsticles. Enhancement of J_c below 60 k is a result of antiferromagnetic behavior of the material. Because of strong interaction between flux lines and nickel ferrite nanoparticles [44].

A. palenzona and A. Sala fined a new approach for the improvement of the critical current density of the Fe ($Se_{0.5}$ $Te_{0.5}$) polycrystalline materials. A new method set for sample is presented which is based on annealing and melting stages. Sintered process creates the densest and homogenous sample. Which is categorized by grain interconnectivity. Such type of samples shows the sharp resistive, magnetic transition, critical temperature, large   hysteresis loop and high upper critical field. Unexpectedly, global critical current density enhanced as compared to bulk sample of the same family. At 4.2 k J_c reached to 10^3 A/cm^2 as measured by magnetic transport also with magnetic optical techniques [45]. Novosel and S. Galic reported the effect of doping magnesium bromide with single magnetic domain of alloy of nickel cobalt bromide, cover and uncoated with $SiO2$. The experiment performed under field and temperature for measurement of critical current density, magnetization and resistivity. Doping in sample gives results of reduction in transition temperature linearly with concentration of dopant atom and intergranular connectivity also decrease with increasing of dopant concentration. Throughout temperature interval, there was reduction in critical fields (irreversible field, upper field) of doped material. On the other hand, at low temperature J_c enhanced in doped material as comparison with undoped material [46].

S. X Dou and Y. Zhao investigated the depressed occur in T_c and J_c by the influence of iron nanoparticles in both the form of bulk and thin film superconductor. MgB_2 wires are manufactured but Iron is a vital material for fabrication of these wires. Influence of iron nanoparticles on the properties of MgB_2 till now debated. TEM and XRD are used for this experiment but there is no iron or iron bromide compound was found in sample at 1% doping. Which consider that iron is resided in lattice of magnesium. Fe level for doping in Mg lattice is occured lower than 1%. Th doping of iron, become cause for reduction in transition temperature. This effect occurs due to high reactiveness of iron at nanoscale. The iron is substituted in the form of FeB at large scale then doping level is 2% which is detected through XRD and TEM. While in form of Fe2B there is doping level 10% which is detected. When doping level increased up to 2% then value of J_c reduced. Fe and Fe_2B have characteristics to weak the connectivity between grains [47].

Wel Gao with john B vander Sande works on the improvement of critical current density by mechanical deformation in superconducting composites of textured BSCCO/Ag. Oxidized the precursor of superconducting composites of BSCCO/Ag to get well defined phase "2223". After that sampling process under the deformation and annealed for required texture of microstructure. The texture phase "2223" orientation along c-axis which is explain by lotgering factor, F. This factor is calculated by X-ray diffraction. Jc was measured under the varying field, to observe the microstructural texture effect on field dependence of critical current density. These observations, explain the relationships between critical current density, degree of c-axis texturing and with deformation process. The micro level study of electron probe and structure were achieved to find the interrelation between microstructure, transport properties and processing parameters. To optimize the annealing with also chemical composition so that to get the well-defined phase "2223" then for purpose of high quality texture creation corresponds to reduction in calcium and copper phases which is non-superconducting in this phase. Magnetic field behavior becomes better from the deformation and texture process of superconducting ribbons. Whereas J_c drops 2% in field of 20 m Tesla of non-texture ribbons as compared to zero fields. Observation shows that there is increase in critical current density from 500 A/cm^2 almost for the non-textured ribbons to 4000 to 10000 A/cm^2 for well textured sample at 77k for field is zero. Research is doing now a day for the further improvement in critical current density and texture [48].

C.V. Varanasi and P.N Barnes studied the flux pinning enhancement in the $YBa_2Cu_3O_{7-\&}$ (YBCO) with $BaSnO_3$ nanoparticles. The material $YBa_2Cu_3O_{7-\&}$ (YBCO) is doped with nanoparticles of the $BaSnO_3$ on substrate of the LaAlO3 for purpose of increasing in critical current density. The value of improvement in high field magnetization J_c at 6 Tesla about 77 k was observed as contrast with film regular in YBCO. The enhancement of critical current was observed in field. When field is 1 T then angular dependence of critical current density which explains that J_c H parallel to c axis higher 1.3 times than J_c H parallel to ab axis which points out that correlated defects along c axis. TEM results show presence of uniform distribution of nano sized BaSnO3 having large density, hastens and stress fields around them. Film was produced by using pulsed laser deposition target. Therefore, reaction performed between $BaSnO_3$ and $YBa_2Cu_3O_{7-\&}$ (YBCO) which is elimination reaction for preparation of target state. Which may permit to react locally and produced defect for acting as pinning center [49].

Mansoor Farbod and Muhammad Reza Batvandi explain the effect of nanoparticles of Ag on current density of the $YBa_2Cu_3O_{7-\&}$ (YBCO) superconductor. Nanoparticles of Ag were prepared by reduction of $AgNO_3$ through chemical reaction in alcohol solution which produced different size of particle ranging from 30 nm to 1000 nm. Then doped the sample with 1 or 2 percent of nanoparticles having different particle size. XRD data analysis gives us phase formation in sample. Whereas SEM results explain the morphology of material. In other hand EDX confirms the composition of each element in sample. Critical current density calculated using method of four probe at temperature of liquid nitrogen. When particle size reached to 700 nm then value of J_c maximum for further increase in particle size there is decrease in value of J_c. The enhancement of J_c confirm that there is strong conductivity between grain boundaries and good crystallization in grains [50].

A.N Jannah and R. Abd-shukor investigated the effect of cobalt oxide nanoparticles on bismuth and lead based superconductor. Coprecipitation method was used for the sample manufacturing. Cobalt oxide with different size having variation in sample. XRD analysis confirm phase formation. Whereas SEM used for microstructural study of sample and EDX gives information about composition of each element in sample. From XRD data confirms that major peak of Bi-2223 and minor peak of Bi-2213. The highest value of volume fraction was obtained in phase Bi-

2223 because of addition of cobalt oxide nanoparticles x= 0.01% wt and high value of T_c in superconducting phase Bi-2223. The added sample show the low transition temperature as contrast to the non-added sample [51].

S.Y.S. Yusainee and H.Azhan explain the effects of Y_2O_3 nanoparticles on the properties of Bi-2212 superconductor. The superconducting material was manufactured by using the solid-state reaction in the powder form containing 0.0 to 1.0% Y_2O_3 nanoparticles to balance the sample before sintering. XRD data analysis the phase formation in sample and SEM was used for information of surface morphology. The value of critical current density measured by using four probe methods. Then sample gives the highest value of transition temperature and Jc as contrast to the pure sample of material [52].

Xueguang Dong and A. Pengfei studied the effect on $YBa_2Cu_3O_{7-\&}$ (YBCO) superconductor by addition of Fe_2O_3 and alpha Fe_2O_3 nanoparticles. Basically, in superconductors the enhancement of critical current density corresponds to the flux pinning in material. For the observation of influence of magnetic iron oxide nanoparticles in composite superconductor, prepared sample with former sintered at various temperatures. There is no change in superconductor transition temperature confirmed by measurement of field cooled to a sample. The sintering of sample at high temperature such as 750° Celsius, in results to enhance the critical current density of the sample as compared to that sample which is not sintered or sintering at low temperature almost 350° Celsius. SEM results confirm the morphology of sample means nanoparticles are resided in interstitial sites of the sample. The grain size of sample increases as sintering temperature increased. Thus, flux pinning enhancement confirms that critical current density enhanced by addition of nanoparticles of iron oxide into sample. Fine structure of the material or sample confirmed by X-ray diffraction. After sintering to high temperature, nanoparticles produced the disorder in local structure of the $YBa_2Cu_3O_{7-\delta}$ (YBCO) superconductor and which is confirmed by near edge structure shown by X-ray absorption. The absorption spectra also reveal the transition of phase from tetragonal to orthorhombic phase. The analysis of experimental data, gives the signal of diamagnetic behavior enhancement. Which enhanced the disorder in local structure attribute the superconductor properties. Whereas addition of Fe_2O_3 nanoparticles causes the phase transition in the cuprates. Thus, superconductivity enhanced by increasing the value of critical current density [53].

Amir Zelati and Ahmed Kompan, reported the influence of magnetic nanoparticles on properties of superconductor and its structure. The Bismuth based superconductor was prepared by sol-gel method which has general formula $Bi_{0.6}Pb_{0.4}Sr_2Ca_2Cu_3O_y$ with addition of xEu_2O_3 nanoparticles where x= 0.0, 0.3, 0.5, 1.0 wt %. The XRD used to give the information about the required phase formation in sample. For morphology of sample SEM was used. The structural characterization was done also with transmission electron microscope (TEM). XRD data reveal that there are two phases coexist in same sample as (Bi, Pb)-2223 and Bi-2212. The structure of the sample is orthorhombic in nature. The calculated data of DC resistivity, critical current density and magnetic susceptibility show that after adding magnetic nanoparticles of Eu_2O_3 in sample, there is increased in critical current density and other superconducting properties of BSCCO superconductor composites. The increased in the value of J_c show that there are grains connectivity increased because of the addition of Eu_2O_3 nanoparticles in BSCCO superconductor. The enhancement of critical current density in superconductor by adding nanoparticles occur at x=0.5 wt. % which improve the superconducting properties of Bismuth based superconductor [54].

H.P Wiesinger and F.M Sauerzopf have done his work for calculation of critical current density from MH loop of superconductor. Consider a constant current density passes through a specific volume. Then calculate the average of the magnetization from the MH loop which is the basic difference than other models. This average magnetization corresponds to the critical magnetic field. Magnetization calculation was done by taking average over the local field, prejudiced by area of current loops. The self-field correction function represents the local field which calculated for geometry of a sample only for one time. There are two cases in which we deal with high temperature superconductors. First of all, consider a flat sample having quadratic cross-section and, in this plane, also isotropic critical current which shows a maximum diamagnetism effect. Second case is the sample having dimension perpendicular the field with high anisotropy in critical field. Analytically performed the calculation of self-field correction because the the thickness taking as zero. In the form of standard anisotropy, calculate the anisotropy critical currents. Critical z current density only evaluated when B>B min. Whereas B min is 0.3 T at 40k to 1.3 T at 5k given magnetization measurements of specific sample. The final results of critical current density were similar to those case for which irreversible magnetization is not considerable. Diamagnetism effect was combined with self-field calculations. Which is differ prominently from normal correction of applied field by sample magnetization [55].

Tetsuo Oka and Yoshitaka Itoh, explain the magnetic properties of Zr- YBCO superconductor composites. The process used for enhancement of mechanical strength of Zr-bearing YBCO sintered superconductor composites. The Phase "123" produced by decomposition of the yttrium-based superconductor which contact with Cu-O plane due to addition of Zr, small amount melts at 970. Thus, partially melting played a vital role in reduction of voids. $BaZrO_3$ precipitate saves the sample from colliding and used to enhance the mechanical properties. The value of Zr at x= 1.0 in YBCO superconductor enhanced the value of delta M_{max} which is derived from MH loop. When amount of Zr is low in YBCO superconductor, Zr precipitates act as pinning center [56].

Chapter no 3

Synthesis and Characterization Techniques

3.1 Synthesis techniques

There are two techniques used for the synthesis of nanoparticles.

1- Top down

2- Bottom up

3.1.1 Top down technique

Nanoparticles are formed. when a bulk material is subjected to under the top down technique. There are number of methods of top down techniques which are used for the preparation of nanoparticles. These are named as lithography, skiving, embossing and ball crushing. Most of the technological applications use these techniques significantly in computer chips consisting at integrated circuits and manufactured by using top down techniques by the method of lithography. Further there are two methods for lithography such as photolithography and electron beam lithography [57]. In electron beam lithography, thin film containing substrate used and photo - resist relay on it. There is a photo mask also on this resist. Then electron beam is applied to this resist by the way of photo mask. Electron beam facing region changed into liquid developer due to breaking of bonds phenomena occur. As a result of this phenomena to get the desired result. Then remove the photo resist by using the annealing process and results into pattern formation. Where as in case of photolithography ultra violet light is used, instead of electron beam [58].

3.1.2 Bottom up technique

Atom by atom grow up technique is used for the formation of nanomaterials. This technique is basically chemical approach for preparation of nanoparticles. There are different methods which are used for bottom up. Given as follow chemical vapor deposition (CVD), physical vapor deposition, electrochemical deposition, coprecipitation, sol gel method and molecular beam epitaxy (MBE). Bottom up approach is better than the top down because in this method nanoparticles prepared with minute number of defects and in number of similar chemical compositions [59].
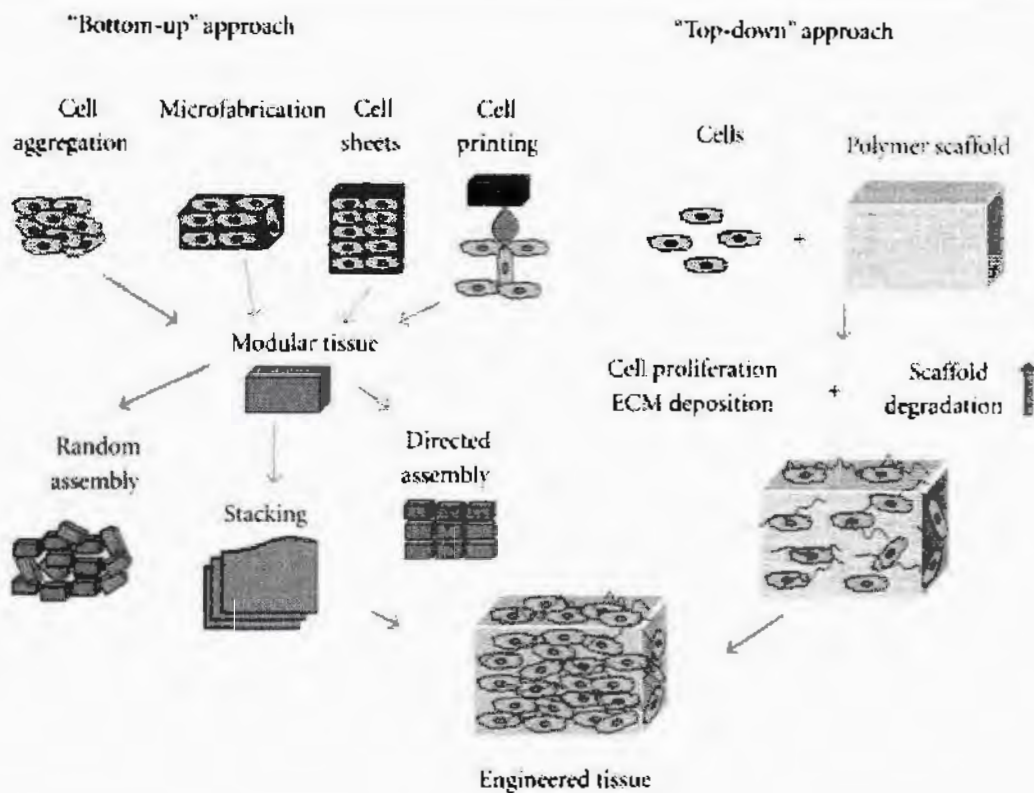
Fig 3.1: Bottom up and Top down [10]

3.2 Sol gel method

This is a wet chemical solution method by which nanoparticles are prepared in the form of precursor. The resulted precursor is a complex form of mixture in which particles are dispersed and cross linked in mixture. The size of nanoparticles in the range of 1 to 100 nm in the form of liquid or solid particles. A sol gel method based on the number of process such as ageing gelation, firing and drying. After these steps required solution formed in which nanoparticles exist as colloidal interruption.

3.2.1 Mixing

The required solution of material is prepared in steps in which mixing is first one step for formation. Colloidal suspension and formation of gelation from solution cause to form gel. This gel led to the inorganic system in this process. For the formation of colloidal suspension, metals were used as precursor. There are two process, hydrolysis and condensation occurred when compounds are mixed into water. Hydrolysis is the reaction of water with a compound. Whereas condensation is the process in which a compound condensed to a stable state. The example of sol gel method to prepare the silica because of the hydrolysis process and polymerization of tetraethyl

silicate. The resulting product of this reaction is silanol with ethyl alcohol. For further condensation and hydrolysis, results to the formation of silicon dioxide.
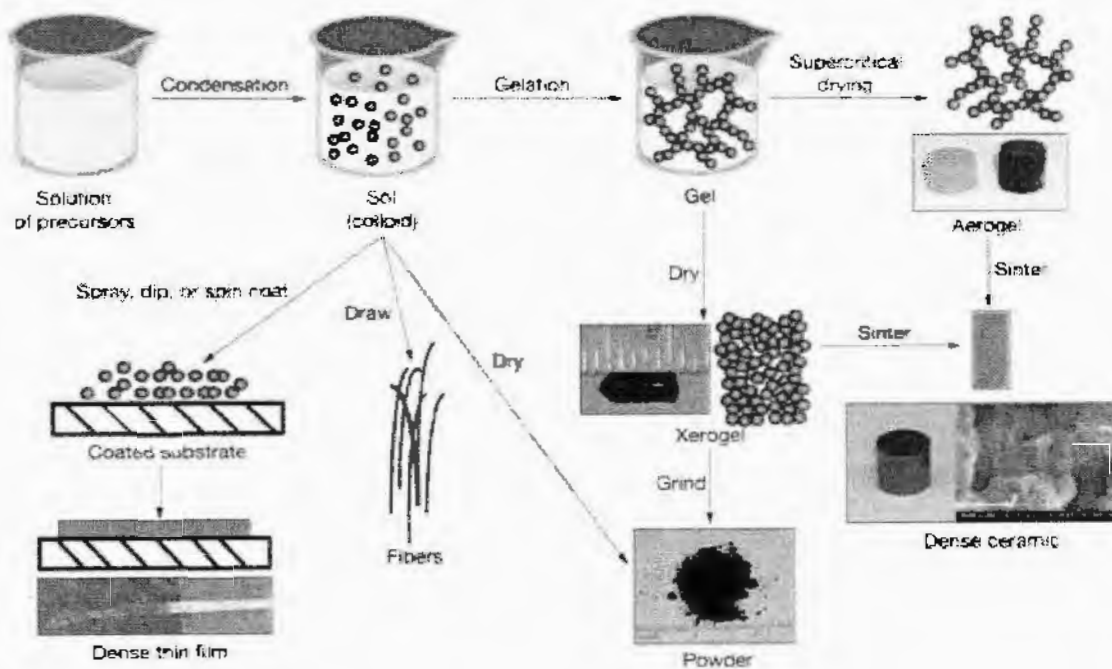

Fig 3.2: Sol gel process[12]

3.2.2 Gelation

Polymers are formed by linking of monomers to each other. Formation of gel with the method to produce the rigidity in solution by homogenous dispersion and this process represents the gelation. Inhomogeneity is forbidden in process of gelation. Properties of sol and gel are same at gel point. There is phase transition from liquid to solid in sol gel process at gel point. In gel process there is in-between state exist [60].

3.2.3 Ageing

There is another step of sol gel process known as ageing. During ageing steps, strengthening the extra cross links to the structure of gel. Gel matrix is manufactured and resulting solution expelled from pores in ageing step. There is change in physical properties during ageing step because of the phase transformation and polymerization [61]. Polymerization phenomena observed in sol gel by varying the catalytic nature, duration of ageing and temperature in molecular precursor. In given solution there were two catalysts used which are non-ionic and ionic in nature.

There observed that duration of ageing shows little bit effect on condensation of atoms in solution [62].

3.2.4 Drying

Gel structure contain the water or other liquids in pores or voids. But in process of drying, liquids are removed from pores which are present in gel structure. This process is carried at temperature of 200 C. After completion of drying process, Xero-gel is formed only when gel is changed into micro pores structure. Aero-gel is formed when dry process is completed in such a way that there is no further breaking in gel network. Two possible ways used for passing the critical point of gel process. One of the process which mostly done before the heating in which used a inert gas to apply the pressure. Autoclave is second process in which volume of liquid added while heating to a gel. Then material formed having property as brittle materials and porous in nature.

3.2.5 Firing

Manufacturing of ceramic material is done by heating to sol-gel at temperature of 400 to 800 °C. In heating phenomenon there is dehydration reactions occur in material [63]. There are various steps which are followed during heating process.

- At temperature of 100 to 200^0 C, there is phenomena of evaporation of liquid and solvents which are absorbed by gel material in pores.
- The phenomena of decomposition of remaining organic compounds occurs at temperature of 300 to 500^{0}C.
- Mostly at high temperature phenomenon of breaking of pores in materials occurred.
- Many other phenomena occurred during sintering and densification such as condensation, surface diffusion and evaporation. At the end, powder form of sample is obtained by grinding a sample. Particle in small size exist in powder form which are become very reactive in nature.

3.2.6 importance of Sol-gel method

Materials formed by this sol-gel method have great importance in different fields. Beside the densification process, temperature is required in all other steps which are included in sol-gel method. Precursor used for the sol-gel method is metal alkoxide which is highly volatile in nature. Solution becomes homogenous when precursor are mixed at molecular level. This method is most suitable to those materials which are of nano-crystalline and pours in nature. Maintain the pH of sample for purpose of securing from sensitive organic materials such as dyes. By using low

temperature and pressure in sol-gel method, nanomaterials are manufactured. Thus, high purity and less size distribution nanomaterials are obtained by sol-gel method [64]. In sol-gel process, use the ageing and drying process to obtain the various size of pores in materials. Different liquids are cooled in sol-gel method to get the glassy solid materials.

The major success of this method to prepare the ceramic materials which cannot be prepared from the conformist powder processing. The resulting gel glasses have similar physical properties with those glasses gained from the melting. In sol-gel method process of hydrolysis gives continuous fibers from metal alkoxide mixture. The powder form of the material is obtained by grinding after process of drying and ageing in sol-gel method. For the purpose of suitable grain size <300 nm, firing the powder form of material then these particles of material known as abrasive particles. Thus, by sol-gel method obtained nanoparticles have wide range of applications. Through Sol-gel method coating of a material and formation of thin film can be possible.

For purpose of coating applications, thickness of the film is small, and process of drying is fast. For coating of a material, there are four possible methods in use which are named as

- Dipping
- Spinning
- Spraying
- Lowering

Sol-gel method is used for different coating of materials such as antireflection coating, filter semiconducting coating, protective layers and self-governing thin film. Thus various types of materials can be manufactured by using sol-gel method because this method is most convenient and suitable for preparation of ceramic materials. Sol-gel method have control on the composition of the chemical materials that is why used in multiple component materials.

3.3 Synthesis of $Cu_{0.5}Ba_2Ca_2Cu_3O_{10-\&}$ Precursor.

Solid state reaction is used for the synthesis of CuTl-1223 ($Cu_{1-x}Tl_xBa_2Ca_2Cu_3O_{10-\delta}$) required superconductor matrix. Firstly, in appropriate ratio, take three compounds copper cyanide, calcium nitrate and barium nitrate. Then mixed these three compounds and for two hours grounded in pestle and mortar. For 12 hours at 860^0C placed the precursor in furnace loaded in quartz boats. Then switched off furnace after 12 hours and when temperature approach to room temperature then open the furnace. Again, ground the sample for two hours and heating again

sample at 860^0C which is loaded in ceramic boats. After this treatment got the final precursor. Thus, synthesis of CuTl-1223 ($Cu_{0.5}Ba_2Ca_2Cu_3O_{10-\&}$) precursor chart shown in the below given
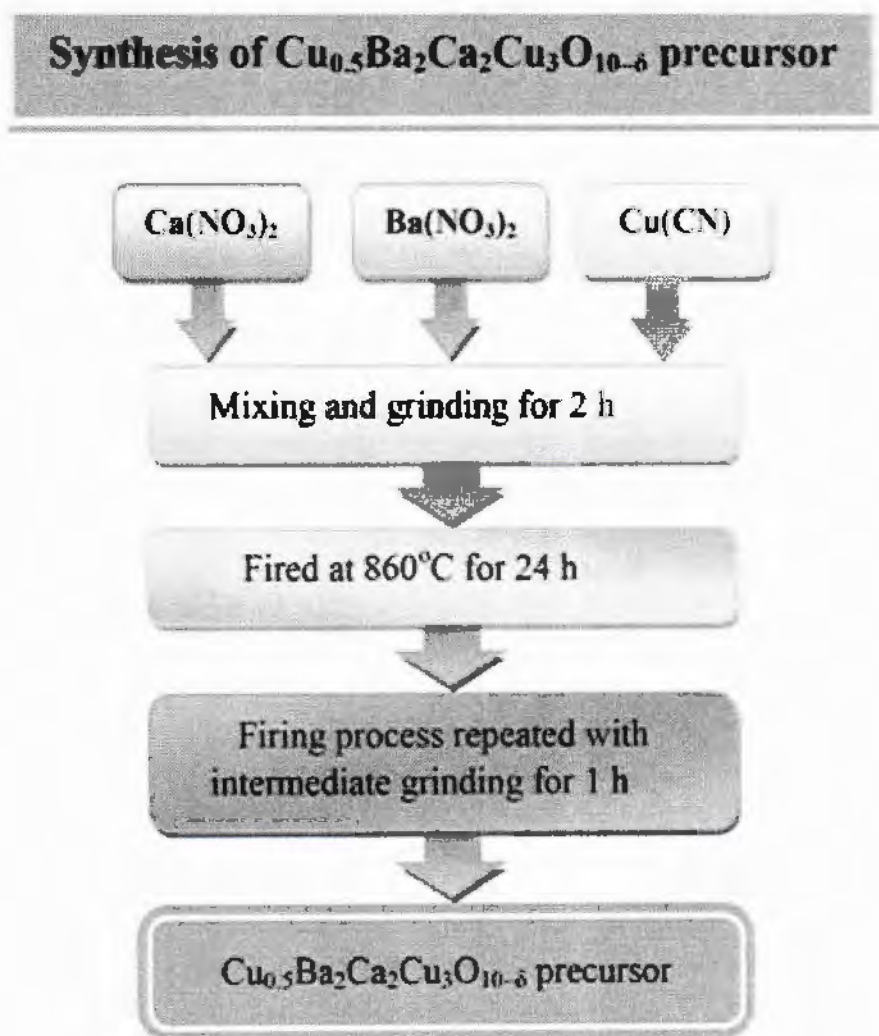

Figure.3.3: Flow Chart of formation of precursor.

3.4 Synthesis of $(Co_3O_4)_x$/CuTl-1223 Superconductor nanoparticles composites

We separately performed the synthesis of cobalt oxide nanoparticles and CuTl-1223 ($Cu_{0.5}Ba_2Ca_2Cu_3O_{10-\&}$) precursor. Then added the nanoparticles of cobalt oxide (Co_3O_4) and thallium oxide with different concentrations in required precursor (x=0, 0.5, 1, 1.5 and 2 wt.%). Then pelletized the sample with the help of hydraulic pressure after grounded the sample for two hours. Pelletized sample placed into the gold capsules and separately sintered at 860^0C for 10

minutes. Thus required sample is synthesized which is $(Co_3O_4)_x$ /CuTl-1223 nanoparticles superconductor composites.
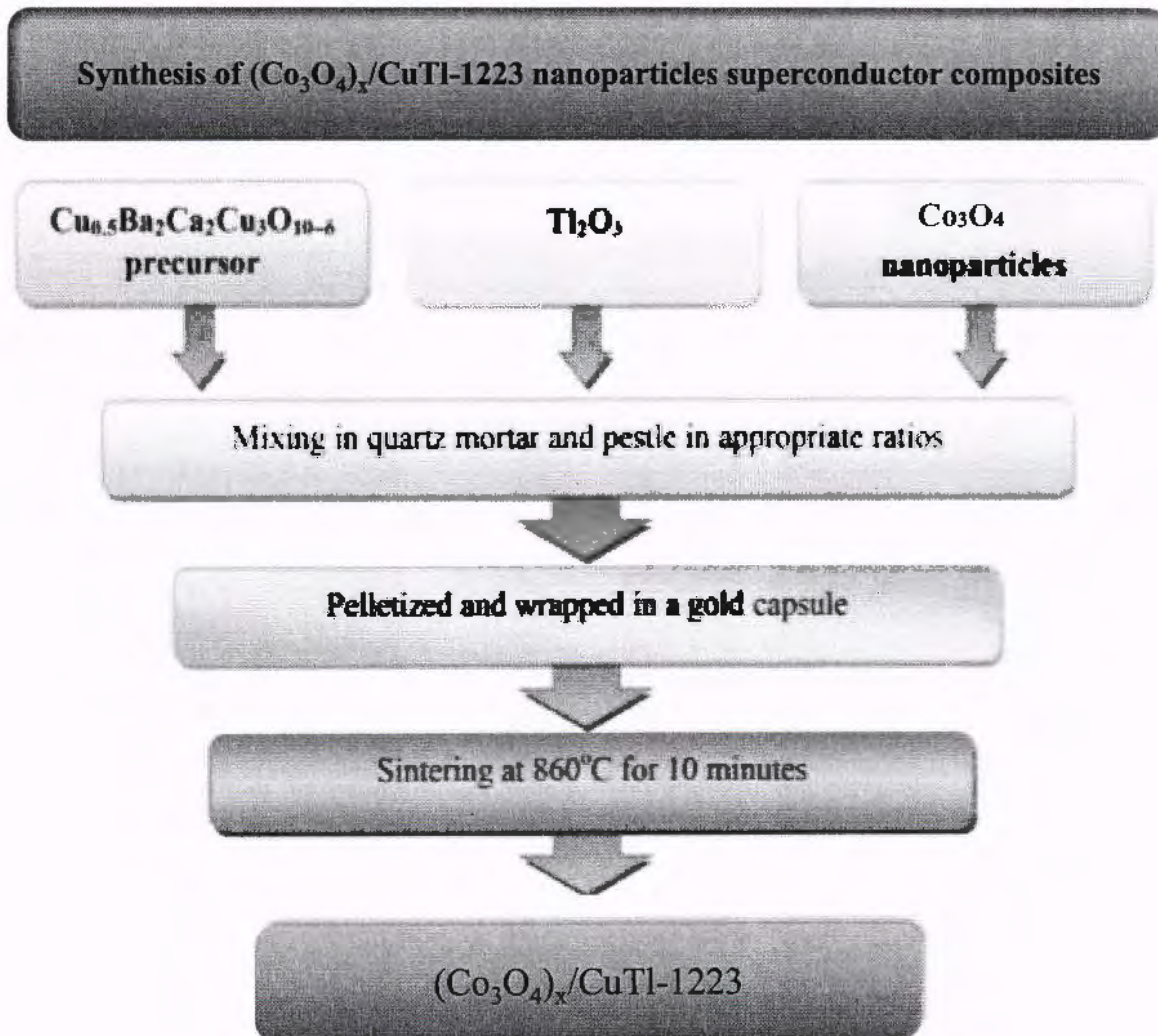

Fig 3.4: Formation of superconductor nanoparticles composites.

3.5 Characterization Techniques

The sample characterized by using the following characterization techniques.

        1-X-rays diffraction (XRD)

        2-Scanning electron microscope (SEM)

        3-Physical properties measurement system (PPMS)

3.5.1 X-ray diffraction

Atoms in any crystal are packed in regular pattern. In crystals, atoms relay in parallel planes in the form of large number of series. For crystal structure information we calculate the distance

between the atoms and planes separation distance. Then other parameters also calculate from this procedure such as cell parameters defects and impurity concentration.

The property of X-rays to infiltrate in to material and diffract from atoms because they have shorter wavelength. Copper is used as the target element for the creation of X-rays in X-ray tube. Wavelength of these created X-rays about is 1.54 Å. The detector identifies the X-rays only when ray is diffracted from atoms of material with an angle θ [65]. Then Braggs law used for calculation of diffraction pattern of X-rays.

3.5.1.1 Basic principle

When X-ray enter into crystal and collide with atoms of crystals then they force to atoms to oscillate about their mean position as shown in figure 3.6. When oscillating frequency of electrons and colliding frequency of ray are identical. There are two types of interference occur which are named as follow.

- Constructive interference

- Destructive interference

Constructive interference possible only when combining rays are in phase or crest fall on crest and trough fall on trough. This type of interference possible only in few directions because of regular arrangement of atoms and it has prominent effect on given sample. Whereas destructive interference occurred only when combining rays are out of phase [66].

3.5.1.2 Braggs law

When lattice constant is greater than wavelength of x-rays then rays diffracted from the atoms of a crystal. But direction of the incident rays is totally different from the diffracted rays. Whenever constructive interference occurred then Braggs law is satisfied for diffraction pattern. Consider interplanar spacing distance d in parallel planes. A X-ray incident on parallel plane and reflected rays have path difference of $2d\sin\theta$. When path difference occurred in the form of integral multiple of wavelength then there is constructive interference.

$$m\lambda = 2d\sin\theta \dots\dots\dots\dots\dots\dots\dots\dots(3.1)$$

Above equation represents the Braggs law for diffracted pattern. The validity of Braggs law is only possible when wavelength is less than or equal to 2d.
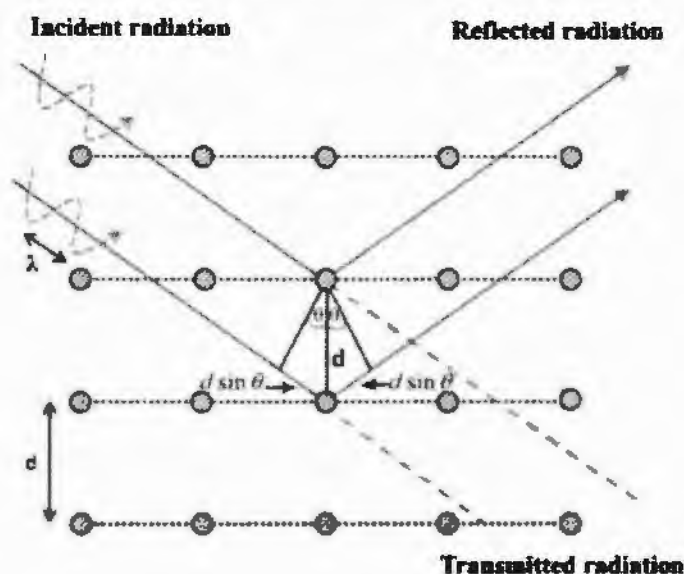
Fig 3.5: X-ray Diffraction[13]

3.5.1.3 Powdered diffraction method

In this method, sample in the form of powder is Subjected to X-rays. The magnitude of angle "θ" changing point to point reflection but in other way value of wavelength "λ" of incident ray remains unchanged. In number of cases, powder diffraction method is used for the classification of superconducting material. Powder diffraction method is also important in other aspect because they give us information about the interplanar spacing, angle of diffracted rays and lattice parameters.

3.5.1.4 Instruments

- **X-ray Generator**

  For production of X-ray a source is used which called as Generator with the help of different types of metals.

- **Goniometer**

  The is a meter on which sample is placed and it works as control the rotation of the sample.

- **Electronic circuit panel**

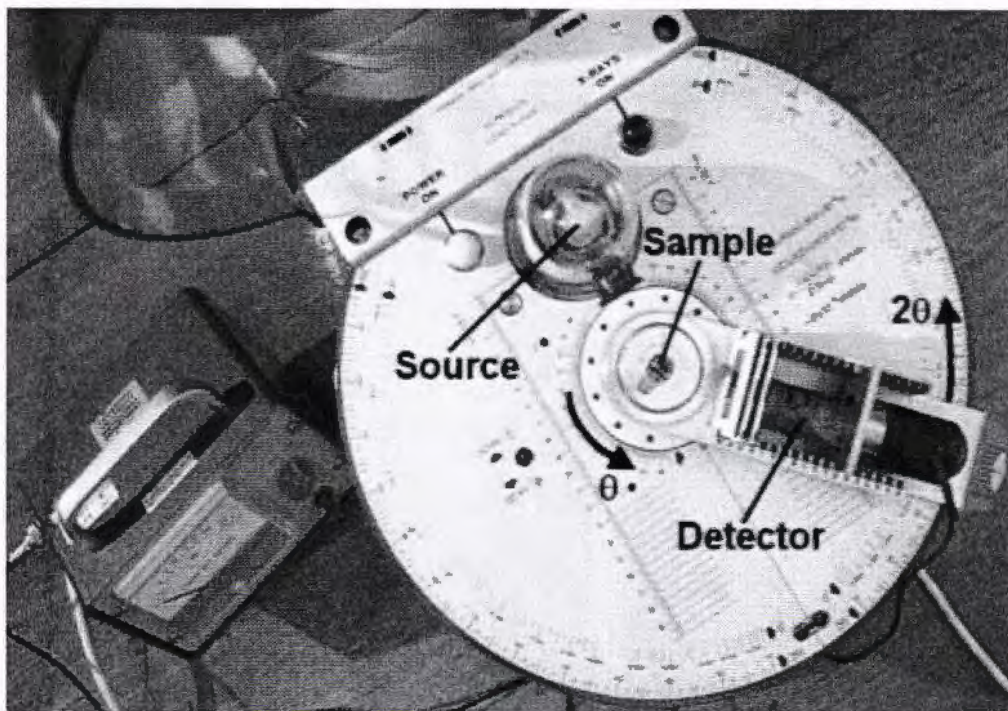 The working of circuit panel to identify and calculate the X-rays [61].

Fig 3.6: X-ray diffraction diagram

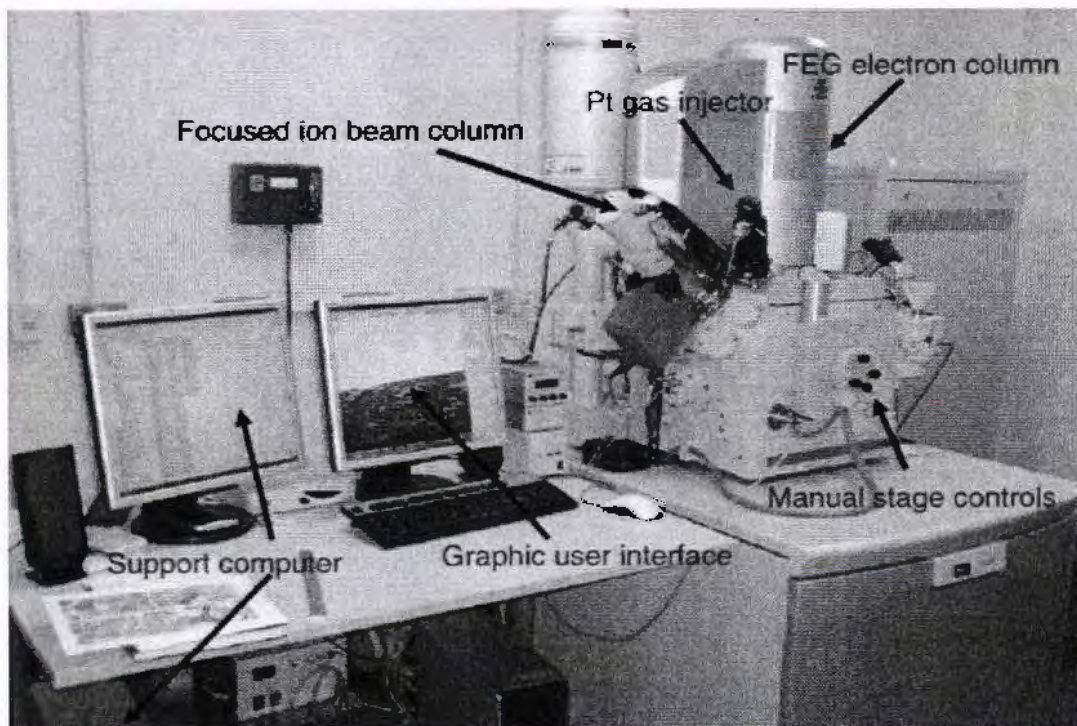## 3.5.2 Scanning electron microscope

Figure 3.7: SEM components[14].

Sample surface morphology is studied by the help of this characterization technique. Because this type machine provides clear image of sample when they scan over the whole surface of the sample

. Its basic working principle is similar as light microscope but difference between them used of source. Light microscope uses the beam of photons as source whereas this SEM use electrons as source. Resolution of the light microscope is lesser than the SEM. In SEM an extra technique used which is name as X-ray energy dispersive spectrometer (EDS). By using this extra technique, Sample surface morphology is studied by the help of this characterization technique. Because this type machine provides clear image of sample when they scan over the whole surface of the sample. Its basic working principle similar as light microscope but difference between them used of source. Light microscope uses the beam of photons as source whereas this SEM use electrons as source. Resolution of the light microscope is lesser than the SEM. In SEM an extra technique used which is name as X-ray energy dispersive spectrometer (EDS). By using this extra technique, which gives the chemical composition of the specimen [67].

3.5.2.1 SEM components

- **Electron gun**

  The purpose of the electron gun to supply the intense electron beam and they fitted at bottom or top of the column. There are two types of electron gun used, one is thermionic gun and other is field emission gun.

- **Lenses**

  Clear and detail image obtained by using the lenses, but functionality of lenses is similar in both SEM and light microscope. Lenses manufactured by using magnets for purpose of focusing the electron beam to target. Thus, this type of lenses called as condenser lenses. Objective lenses which also used in SEM for purpose to control the size of the beam which collide with the surface of material.

- **Chamber**

  Chamber is a place where required sample under study, still position of sample is compulsory for clear and detail image. That's why kept the chamber from any type of vibration. The SEM usually placed at ground level due to its high sensitivity. Angle of the sample can be varied with the help of chamber.

- **Detector**

Electron beam is reflected after the collision with atoms of a crystal. Then these electrons are identify by detector because reflected beam of electrons contain the information of sample morphology. Everhart-Thorny detector used to sense the secondary electrons. Whereas BSE and X-ray detector used for composition of sample [68].

3.6 Vibrating sample magnetometer (VSM)

Magnetic properties are measured by using the technique of vibrating sample magnetometer(VSM). Magnetization basically is response of any type of magnetic material to applied external field. In vibrating sample magnetometer, sample produce magnetization when they placed under the uniformly applied magnetic field. After getting magnetization sample start vibration and produce perturbation also in applied field. Induced perturbation is calculated by the help of fitted number of coils or magnetic field sensors surrounding the sample. In VSM, value of electro motive force in magnetic coils changing because of the change in magnetic flux by perturbation in applied field. The electro motive force in coils depends upon following factors.
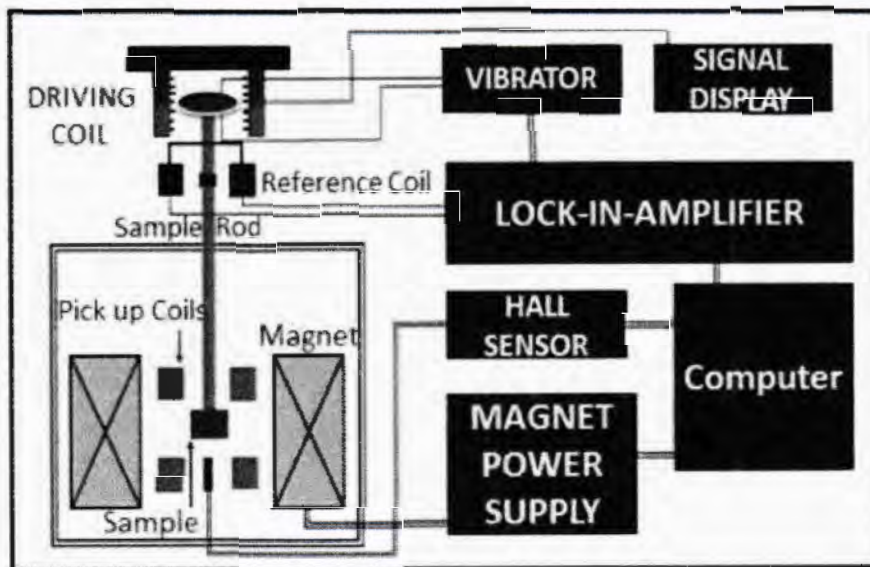

Fig 3.8: Schematic diagram of Vibrating sample magnetometer

1-Magnetized specimen

2-Amplitude of vibration

3-Applied field

4-Frequency vibration

From the induced electro motive force, measure the value of magnetization in suitable handling. Magnetic susceptibility can also measure by the help of VSM in suitable temperature. Given specimen is vibrated under controlled amplitude in VSM. To magnetize the specimen with help of electromagnets the perturbation in applied field generated by the vibration of sample, collected by using superconducting coils [71].

Chapter no.4

Results and Discussion

4.1 XRD   analysis

The X-ray diffraction pattern of cobalt oxide nanoparticles shown in Fig. 4.1. All diffraction peaks are well indexed according to face center cubic structure of nanoparticles of cobalt oxide [72]. In given graph, well defined peaks also show that the crystallinity of sample is good. Debye Scherrer's formula is used for calculation of crystallite size of sample. Thus, average crystallite size obtained from this formula is 71nm. There are some minor peaks which is due to the presence of impurity in sample.
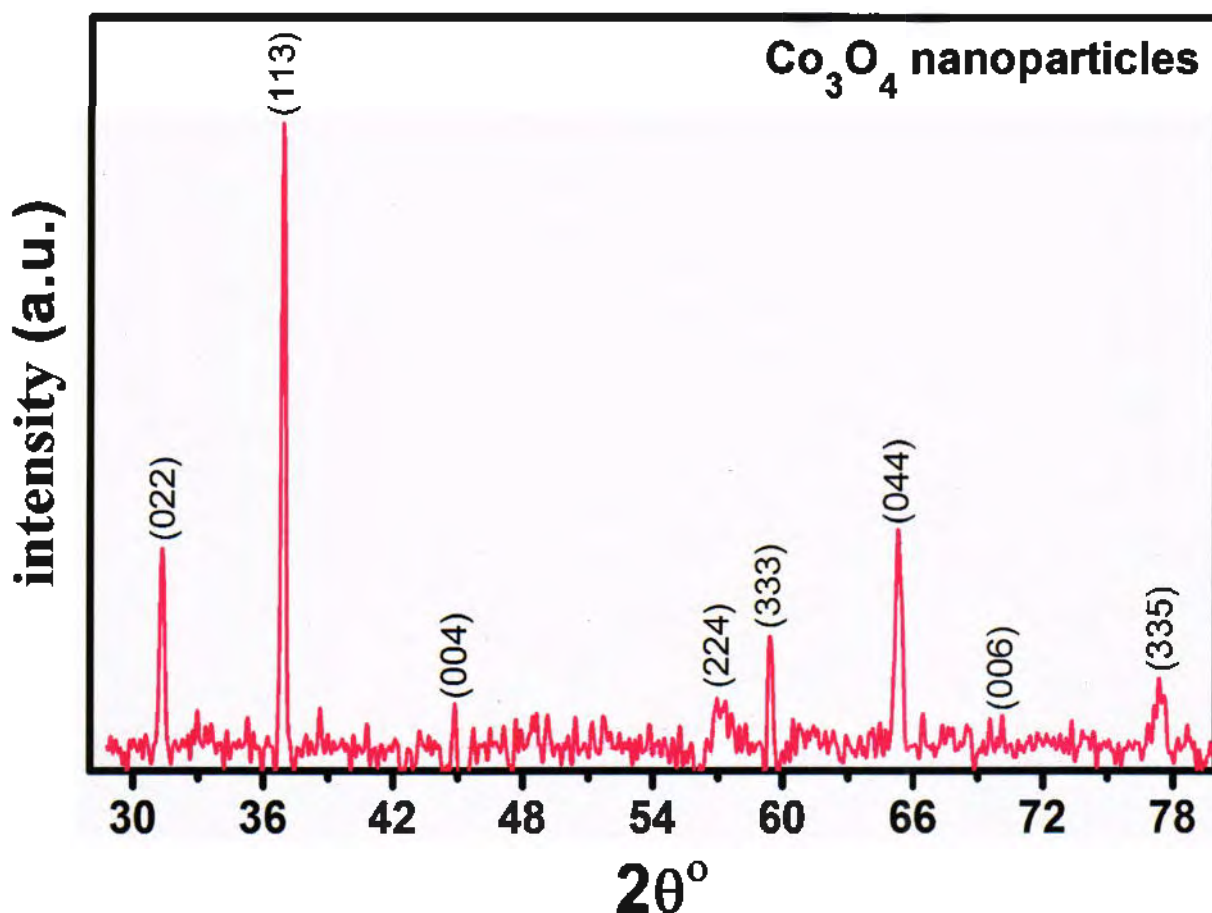

Fig. 4.1. XRD spectrum of Co3O4 nanoparticles

XRD patterns of polycrystalline material $(Co_3O_4)_x$/CuTl-1223 nanoparticles-superconductor matrix with x= 0 and x = 2.0 wt. % is shown in Fig. 4.2. In given figure, bottom pattern of peaks represents material with x=0 wt. % and above pattern of peaks show the material with x = 2.0 wt. % cobalt oxide nanoparticles concentration. In figure 4.2 mostly diffracted peaks in both spectra are well index according to CuTl-1223 tetragonal structure followed by the symmetry of p4/mmm. Both these patterns contain some minor peaks due to the impure phase of CuTl-1223 and few other unknown impurities For both spectra of peaks of $(Co_3O_4)_x$/CuTl-1223 , lattice parameters are determined with x=0 wt% are a=b= 4.1Å, c=15.7Å and with x=2.0 wt. % are a=b= 4.5Å, c=15.4Å. There are small variation in lattice parameters which is due to stress and stain produce by the nanoparticles at grain boundaries. The phase of CuTl-1223 material after addition of Co_3O_4 remain unchanged which reveals that nanoparticles are dispersed into the material grain boundaries.
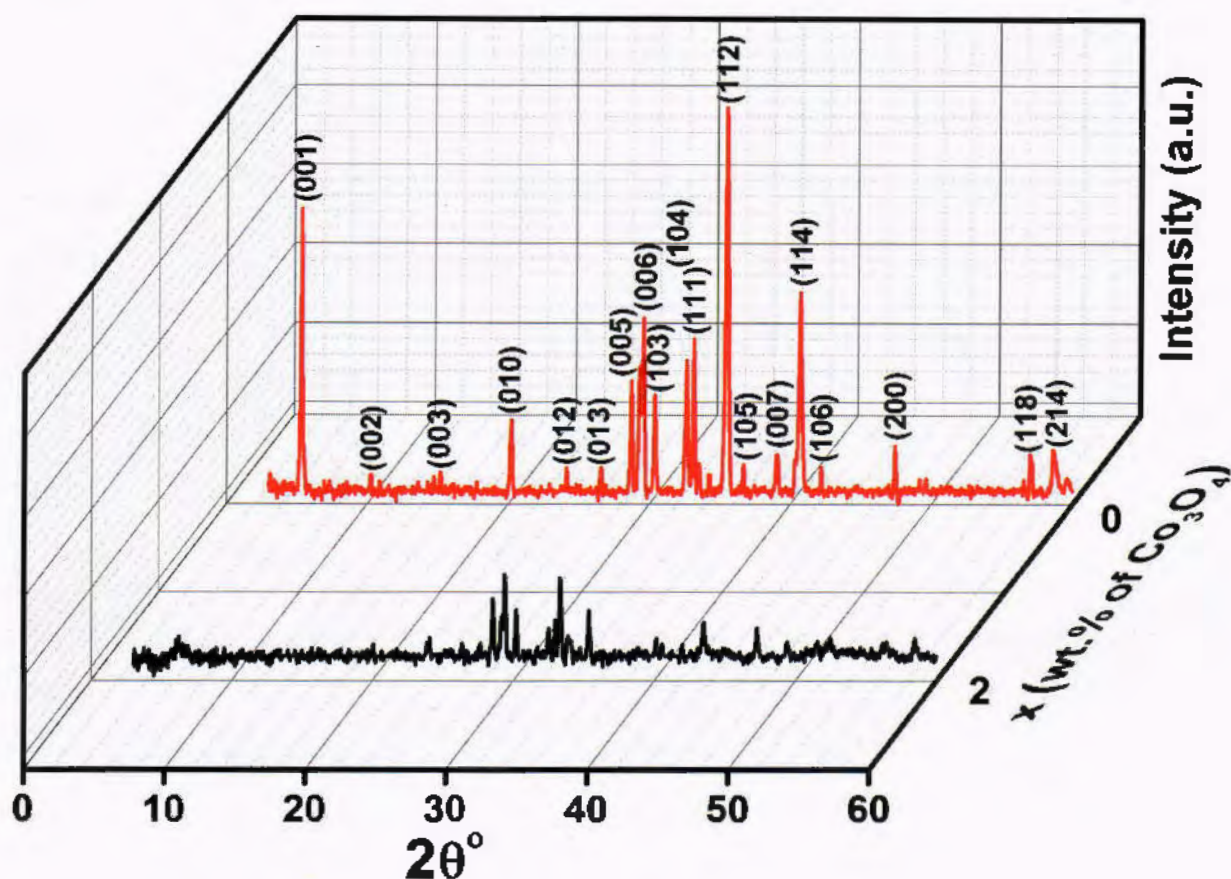

Fig. 4.2. XRD spectra of $(Co_3O_4)_x$/CuTl-1223; x = 0 and 2.0 wt.% nanoparticles-superconductor composites.

4.2 M-T curves

Fig 4.3 (a-e) gives us information about measurement of field cooled (FC) and zero field cooled (ZFC) of $(Co_3O_4)_x$ /CuTl-1223 nanoparticles-superconductor composites at x=0 ,0.25, 0.5, 1 and 2 wt% in the temperature range of 5k to 300k. The zero field cooled curves (ZFC) shows the onset temperature $T_c^{(onset)}$ (K) of diamagnetic transition, which are round about 110K, 109K, 102K, 95K and 81K for x=0, 0.25, 0.5,1 and 2 wt% respectively. The $T_c^{(onset)}$ (K) temperature is taken at a point from which both field cooled (FC) and zero field cooled (ZFC) curves starts emerging. In other words, $T_c^{(onset)}$ (K) is the temperature from which superconducting state growing in a material. The zero field curves brief that addition of nanoparticles results in suppression of $T_c^{(onset)}$ (K) temperature of $Co_3O_4)_x$ /CuTl-1223 nanoparticles-superconductor composites. suppression in $T_c^{(onset)}$ (K) temperature of material show that addition of nanoparticles could not produce inter-grain connectivity. Addition of nanoparticles fill up the pores and voids in material in spite of that they did not create inter-grain connectivity. Thus, addition of nanoparticles produces a repulsive force between grain boundaries and $T_c^{(onset)}$ (K) start to decrease gradually. Thus, in figure 4.3(f) show the decrease in $T_c^{(onset)}$ (K) with increase in concentration of ferromagnetic ordering nanoparticles. The values of $T_c^{(onset)}$ (K) in zero field cooled and field cooled magnetization measurement observed to be slightly less than the values of $T_c^{(onset)}$ (K) in R-T measurement [74]. Which is attributed to fact that percolation plays a vital role in measurement of transport properties. Before approaching to $T_c^{(onset)}$ (K) sample resistivity start decreasing which is due to percolation of superconductivity [75]. The measurement of Field cooled curves done under the field of 0.01T. All Field cooled curves do not show typical Meissner signal during its measurements.

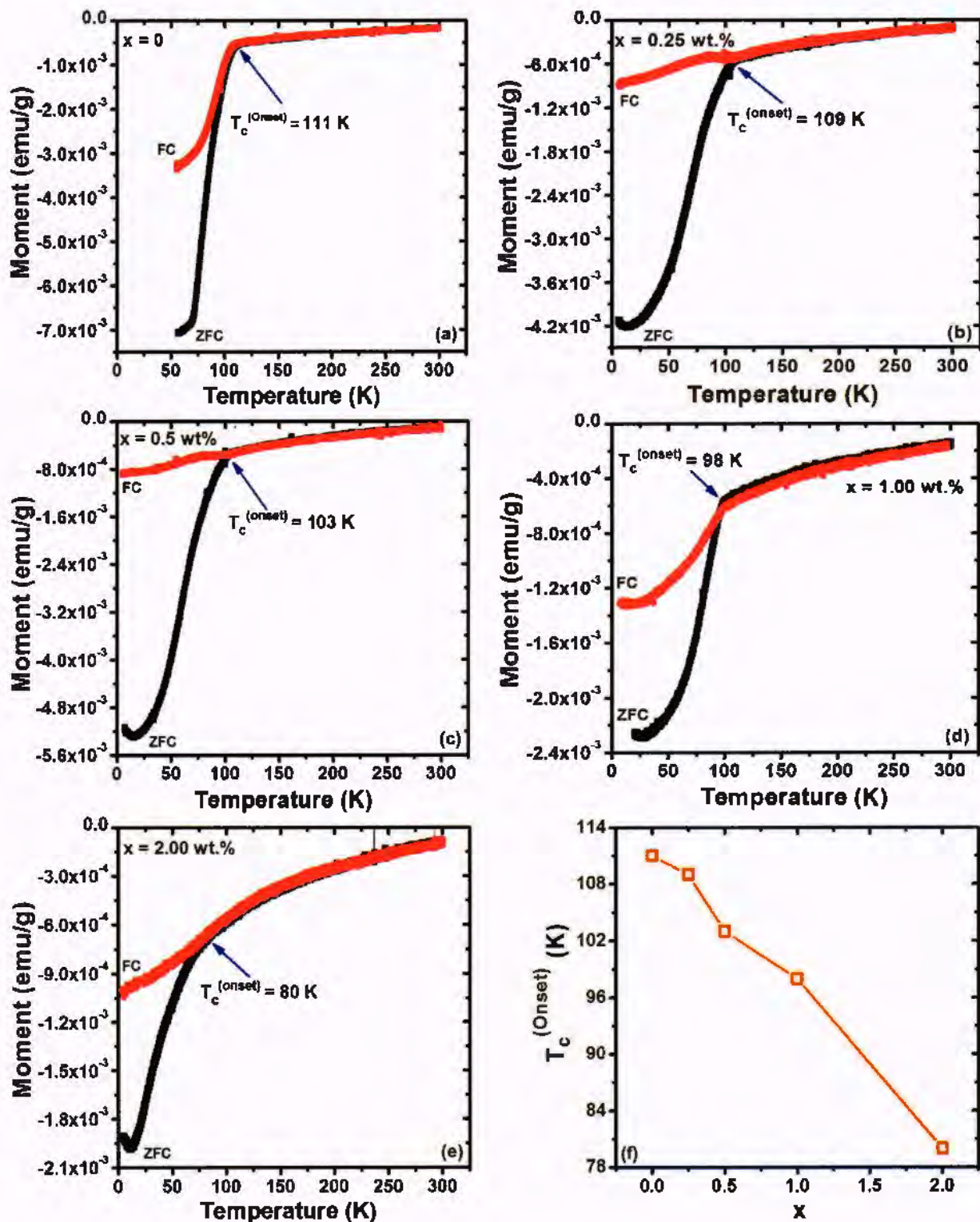**Fig. 4.3(a-f).** Zero field cooled (ZFC) and field cooled (FC) measurements of magnetic moment versus temperature (M-T) for $(Co_3O_4)_x$/CuTl-1223 nanoparticles-superconductor composites with (a) x = 0, (b) x = 0.25 wt.%, (c) x = 0.50 wt.%, (d) x = 1.00 wt.%, (e) x = 2.00 wt.% and (f) Variation of T_c^{Onset} (K) versus x (wt.% of Co_3O_4 nanoparticles).

4.3 Magnetic Hysteresis

MH loops of $(Co_3O_4)_x$/CuTl-1223 sample shown in figure 4.4(a-h). These MH graphs in which field applied between -6Tesla to 6Tesla at different temperatures of 5K,20K,40K,60K,80K.100K,120K and 150K . MH loops of sample with concentration of nanoparticles as x=0%, 0.25%, 0.5%, 1% and 2 wt%) shown in eight different graphs. Each graph contains information about magnetization of sample by varying nanoparticles concentration and field against the specific temperature. MH curves depict that there are suppression in magnetization and area of the loop becomes narrow with increasing of temperature. Sample diamagnetic behavior changes into paramagnetic with increase of temperature. Whereas at high temperatures of 100K, 120K and 150K magnetic behavior changed from diamagnetic to paramagnetic because of sample starts to change from superconducting to normal state. At high temperatures such type of behavior expected because of thermal fluctuations take place and resistivity becomes greater as a results pairing rate becomes lesser than de-pairing rate. As increase in concentration of nanoparticles there are decrease in width of MH loop which is due to enhancement of scattering cross section of electrons in superconducting phase across over the nanoparticles
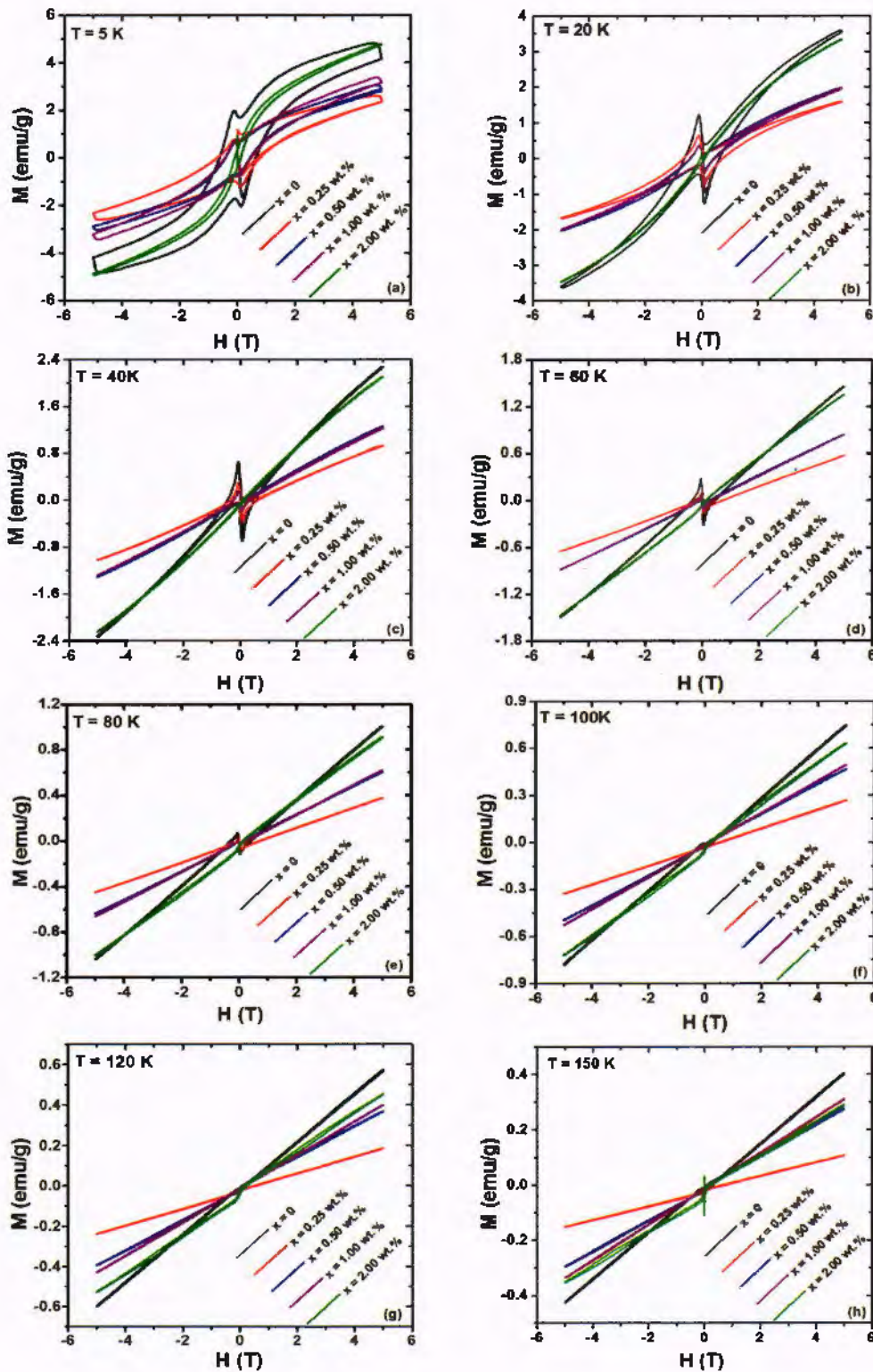
Fig. 4.4(a-h). Magnetic hysteresis (M-H loops) curves of $(Co_3O_4)_x$/CuTl-1223; x = 0, 0.25, 0.50, 1.00 and 2.00 wt.% nanoparticles-superconductor composites at temperatures of 5 K, 20 K, 40 K, 60 K, 80 K, 100 K, 120 K and 150 K.

4.3: Critical current density measurement

The J_c value was observed to be gradually increased with increasing magnetic field (H) up to certain level i.e. H < 0.3 T followed by decreases in value of J_c. The increasing of J_c value with increasing H in the low field area is the features of Bean's model. At low field the number of vortices are less than the pinning centers, thus J_c increases with increase in H (in the presence of week magnetic field). This region is inconsistent with the Kim and Aderson model, according to which J_c should decrease with increasing H. Above H > 0.3 T .A systematic decreases in J_c was observed with increasing H. It can be observed from the graphs that J_c of the host CuTl-1223 matrix decreases with addition of Co_3O_4 nanoparticles which shows the enhanced flux de-pinning of host matrix with addition of nanoparticles. . The flux pinning suppressed with the addition of nanoparticles which may be credited to the enhancement in inter-grains connectivity of host matrix by dispersion of ferromagnetic Co_3O_4 nanoparticles over grain boundaries [69]. The grain boundaries observed to be natural pinning sites in high temperature superconductors, but when ferromagnetic ordering containing nanoparticles occupy these areas a repulsive force is created between magnetic vortices and grain boundaries. Due to which the flux dynamics enhanced inside superconducting grains. According to the power law; $J_c = \beta H^{-\alpha}$, the experimental data of J_c versus H curves were fitted which is the representative of TAFF region [70]. The fitting lines along with the experimental data at 5 K and 20 K for two representative $(Co_3O_4)_x$/CuTl-1223 composites with x = 0 (pure CuTl-1223 superconductor) and with x = 1.00 wt. % are shown in Fig.4.5. The experimental data and fitted lines are in good agreement as shown in Fig. 5. The value of α in above mentioned power law gives the suppression rate of J_c with increasing H. The values of α obtained for $(Co_3O_4)_x$/CuTl-1223 nanoparticles-superconductor composites with x = 0 and 1.0 wt.% at 5 K are 0.50129 and 0.48723, respectively. Similarly the values of α obtained for $(Co_3O_4)_x$/CuTl-1223 composites with x = 0 and 1.0 wt.% at 20 K are 1.04239 and 0.90423, respectively. By comparing these values of α, it can be observed that the addition of Co_3O_4 nanoparticles in CuTl-1223 superconducting matrix has lowered the decreasing rate of J_c with increasing H. This fact makes Co_3O_4 nanoparticles added CuTl-1223 superconductor suitable for high field applications, like superconducting magnets used in particle accelerators. Similar effects of Co_3O_4 nanoparticles' in different superconducting matrices have already been reported in literature [76]. Dependence of J_c on H according to above said power law was not observed for

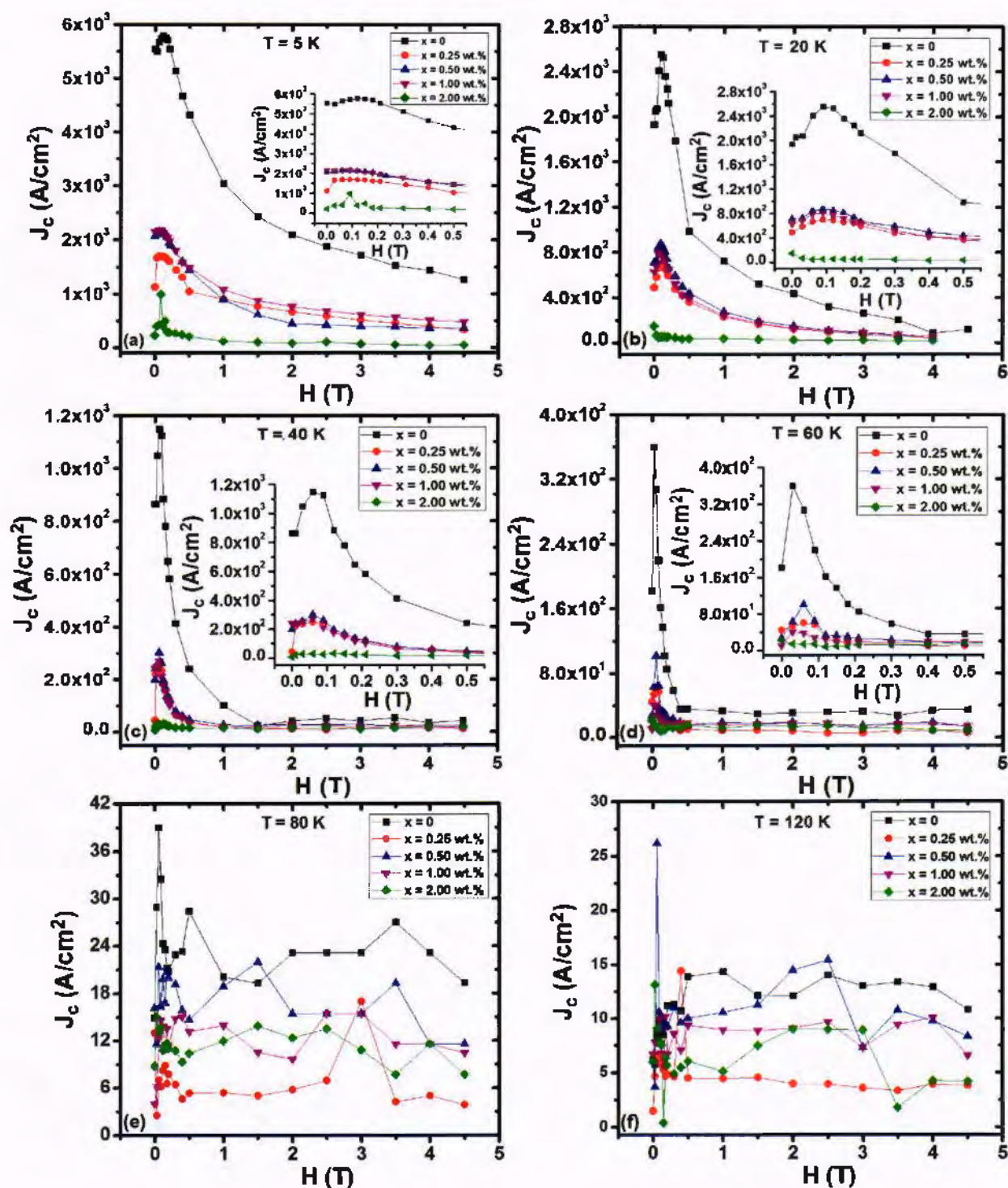**Fig. 4.5(a-f).** Field dependent critical current density (J_c) of $(Co_3O_4)_x$/CuTl-1223; x = 0, 0.25, 0.50, 1.00 and 2.00 wt.% nanoparticles-superconductor composites at temperatures (a) 5 K, (b) 20 K, (c) 40 K, (d) 60 K, (e) 80 K and (f) 120 K. In the insets of Fig. 5(a-d) are shown the variation of J_c versus H in the range of H = 0 to 1 T.
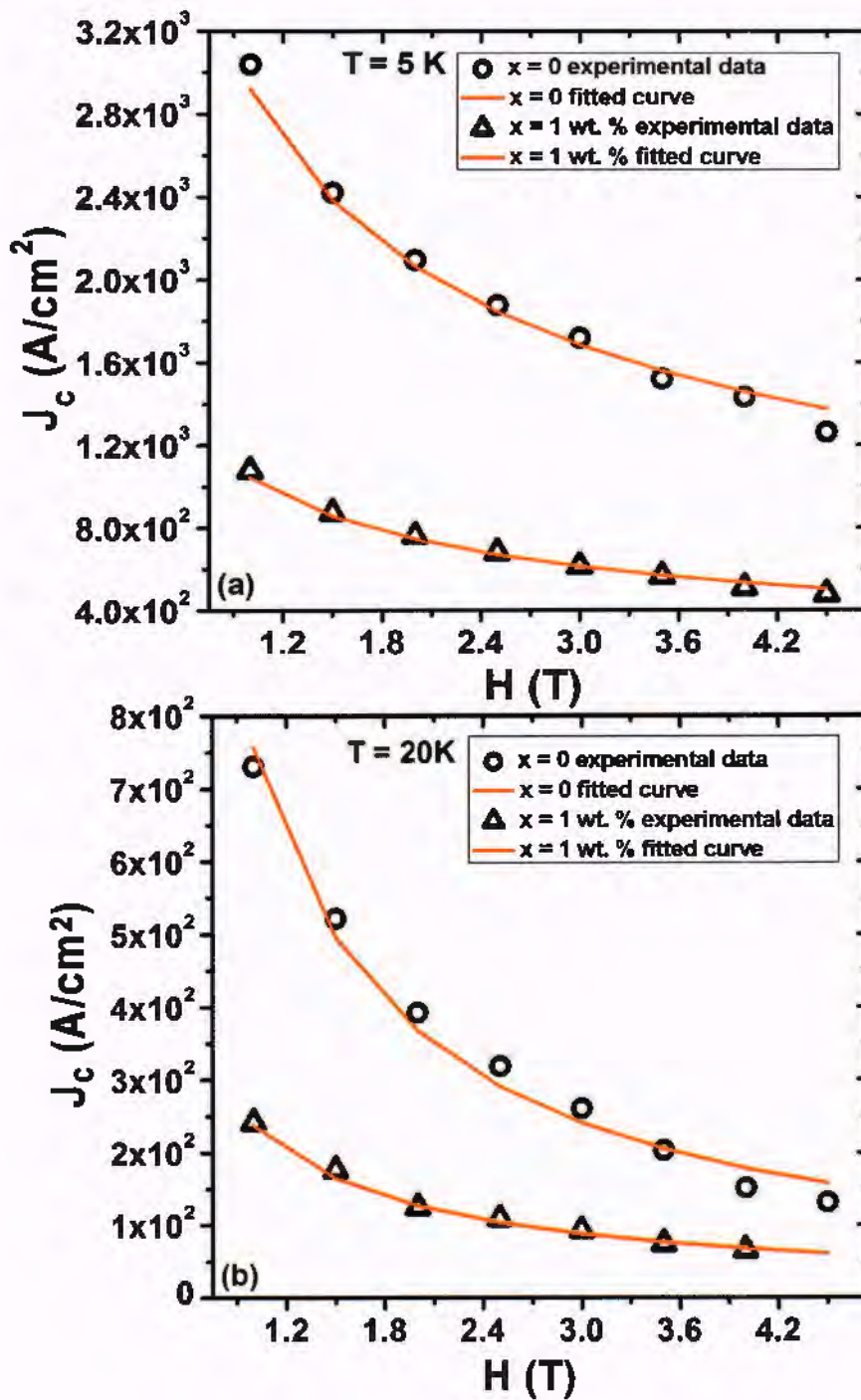
Fig. 4.6. Fitting of critical current density (J_c) versus H of $(Co_3O_4)_x$/CuTl-1223; x = 0 and 1.0 wt.% nanoparticles-superconductor composites at temperatures of 5 K and 20 K according to power law $J_c = \beta H^\alpha$.

higher temperatures, which may be due to transformation of thermally activated flux flow (TAFF) region to free flux flow region (FFF).

4.4 Conclusion

The effects of magnetic Co_3O_4 nanoparticles' addition on infield transport properties of CuTl-1223 superconducting phase was investigated. The invariant crystal structure of host CuTl-1223 superconducting phase after addition of these Co_3O_4 nanoparticles showed the successful dispersion of these nanoparticles at inter-granular sites of host CuTl-1223 superconducting matrix. T_c^{Onset} (K) for the CuTl-1223 superconductor was observed to be decreased with the addition of Co_3O_4 nanoparticles. The values of J_c of $(Co_3O_4)_x$/CuTl-1223; x = 0, 0.25, 0.50, 1.00 and 2.00 wt.% nanoparticles-superconductor composites were calculated from M-H loops by using Bean's model. The addition of Co_3O_4 nanoparticles having week ferromagnetic ordering has enhanced the flux de-pinning in the host CuTl-1223 superconducting matrix. Despite of suppression in flux pinning strength of host CuTl-1223 matrix, Co_3O_4 nanoparticles' addition has enhanced the sustainability of J_c with increasing magnetic field at lower operating temperatures.

References

[1] H.K Onnes and A.Van .Wetenschappen (Amsterdam) **14,**113 (1911).

[2] M. Tinkham "Introduction to superconductivity" 2nd Ed. Dover Publications (2004).

[3] H.K Onnes Commun Phys. Lab.**12,** 120 (1911).

[4] W. Meissener and R. Ochsenfeld , Nat. Sch. **21,**787 (1933).

[5] J. Bardeen, L. N. Cooper and J.R Schrieffer, Phy. Rev. **108,** 1175 (1957).

[6] M. L. Chu, H. L. Chang, C. Wang, J.Y. Juang, T.M. Uen and Y.S. Gou, Appl. Phy.Lett.**55,** 188 (1986).

[7] J.G .Bednorz and K.A Muller, Zeit.Phys.**64,** 189 (1986).

[8] K. Heine, J. Tenbrink and M. Thoner, Appl. Phys. Lett.**55,** 2441 (1989).

[9] D. Dew-Hughes, "The critical current of superconductors: an historical review" J. Low Temp. Phys. **27,** 967 (2001).

[10] N. Hosseini, S. Kananian, A. Zabetian, and M. Fardmanesh, "Point contact based method to measure critical current density of superconductor bulk" Phys. Procedia **36,** 655 (2012).

[11] H. Froehlich, "Theory of the superconducting state " Phys. Rev. **79,** 845 (1950).

[12] A. A. Abrikosov, "Magnetic properties of superconductors of the second group", Sov. Phys. JETP (Engl. Transl.) **5,** 1174 (1957).

[13] D. M. Ginsberg," Physical properties of high temperature superconductors III", World Scientific (1992).

[14] C. Gorter, "On the possibility of a dynamic variety of the intermediate superconductive state", Physica **23,** 56 (1957).

[15] A. Saleem, S.T. Hussain, Review the High Temperature Superconductor (HTSC) Cuprates Properties and Applications, J. Surf. Inter. Mat. **1,** 119 (2013).

[16] T. Watanabe, S. Miyashita, N. Ichioka, K. Tokiwa, K. Tanaka, A. Iyo, Y. Tanaka and H. Ihara, Carrier doping and superconducting properties in Cu-1234 and CuTl-1223 superconductors, Phy. B **288,** 1076 (2000).

[17] K. Tanaka, A. Iyo, N. Terada, K. Tokiwa, S. Miyashita, Y. Tanaka, T. Tsukamoto, S. Agarwal,T. Watanabe and H. Ihara, "Tl valence change and Tc enhancement (> 130 K) in (Cu,T l)$Ba_2Ca_2Cu_3O_y$ due to nitrogen annealing", Phys. Rev. B **63,** 064508 (2001).

[18] H. Adrian, W. Assmus, A. Höhr, J. Kowalewski, H. Spille, and F. Steglich, Physica C **329,**164(1989).

[19] N. Kobayashi, H. Iwasaki, S. Terada, K. Noto, A. Tokiwa, M. Kikuchi, Y. Syono, and Y.Muto,PhysicaC,**1525**,155(1988).

[20] T. Worthington,W. J. Gallagher, and T. R. Dinger, Phys. Rev. Lett. 59,1160(1987).

[21] A. Schilling, O. Jeandupeux, S. Buchi, H. Ott and C. Rossel, Physica C, **229**, 240 (1994).

[22] M. J. Rice and Y. R. Wang, Phys. Rev. B**37**, 5893 (1988).

[23] Y. Li, X. Fan, J. Qi, J. Ji, S. Wang, G. Zhang, and F. Zhang, "Gold nanoparticles graphene hybrids as active catalysts for Suzuki reaction" Mater. Res. Bull. **45**, 1413 (2010).

[24] G. Schmid, and B. Corain, "Nanoparticulated gold: syntheses, structures, electronics, and reactivities" Eur. J. Inorg. Chem, 2003, 3081 (2003).

[25] A. K. Gupta, and M. Gupta, "Synthesis and surface engineering of iron oxide nanoparticles for biomedical applications" Biomater. **26**, 3995 (2005).

[26] V. Radmilovic, "Advanced imaging and biomedical applications of nanomaterials", J. Serb. Soc. Comput. Mech. **5**, 24 (2011).

[27] M.D Simon and A.K Geim ,"Diamagnetic levitation, Flying frog and floating magnetics" **9**,87 (2000).

[28] Xing LuoYanhui WuManguiHan and LongjiangDeng, "High frequency permeability of Fe-Cu-Nb-Si-B nanocrystalline flakes with the distribution of shape anisotropy fields" **5**,451 (2018).

[29] Winner science "Properties of paramagnetic materials" **5**, (2011).

[30] P. D. C. Burda, "Metallic Nanomaterials" J. Am. Chem. Soc. **131**, 6642 (2009).

[31]www.ndecd.org/EducationResources/CommunityCollege/MagParticle/Physics/HysteresisLoop.htm

[32] C.P Bean, " Magnetization of hard superconductor" Phy.rev.lett. **8**,250 (1962).

[33] H. E. Cline, C. S. Tedmon, Jr., and R. M. Rose, "Irreversible Magnetization of High-Field Superconductor" Phy.rev.lett **137**, (1767).

[34] A A. A. Abrikosov, "On the magnetic properties of superconductors of the second group" Sov. Phys. JETP 5 (1957) 1174.

[35] U. Essmann, and H. Trauble, "The direct observation of individual flux lines in type II superconductors" Phys. Lett. A 24 (1967) 526.

[36] P. Gammel, D. Bishop, G. Dolan, J. Kwo, C. Murray, L. Schneemeyer, and J. Waszczak, "Observation of hexagonally correlated flux quanta in YBa2Cu3O7" Phys. Rev. Lett. 59 (1987) 2592.

[37] A. Moser, H. Hug, I. Parashikov, B. Stiefel, O. Fritz, H. Thomas, A. Baratoff, H. J. Güntherodt, and P. Chaudhari, "Observation of single vortices condensed into a vortex-glass phase by magnetic force microscopy" Phys. Rev. Lett. 74 (1995) 1847.

[38]] P. E. Goa, H. Hauglin, M. Baziljevich, E. Ilyashenko, P. L. Gammel, and T. H. Johansen, "Real-time magneto-optical imaging of vortices in superconducting NbSe2" Supercond. Sci. Technol. 14 (2001) 729.

[39] A. Larkin, and Y. N. Ovchinnikov, "Pinning in type II superconductors" J. Low Temp. Phys. 34 (1979) 409.

[40] G. Kırat a , O. Kızılaslan b , M.A. Aksan, "Effect of the Er-substitution on critical current density in glass-ceramic Bi2Sr2Ca2(Cu3-xErx)O10+δ superconducting system" **42**,15072 (2016).

[41] X.Z. Zhou , H.P. Kunkel, P.A. Stampe , J.A. Cowen , Gwyn Williams, "Field and temperature dependent transport and magnetic properties of superconducting YNi 2 BaC" **251**,183(1995).

[42] Aima Ramli and Hussain "Structural and electrical properties of YBCO added with Nd2O3, Gd2O3 and Sm2O3 nanoparticles", (2015).

[43] Pankaj P. Khirade , Shankar D. Birajdar , A.B. Shinde , K.M. Jadhav, "Room temperature ferromagnetism and photoluminescence of multifunctional Fe doped BaZrO3 nanoceramics" **691**,287(2017).

[44] M. Hafiz and R. Abd-Shukor, "Effect of Nanosized NiF2 Addition on the Transport Critical Current Density of Ag-Sheathed (Bi1.6Pb0.4)Sr2Ca2Cu3O10 Superconductor Tapes" ,5 (2015).

[45] A.Palenzona1,3, A.Sala1,2, C. Bernini3 , V. Braccini3 , M.R.Cimberle4 , C.Ferdeghini, "A new approach for improving global critical current density in Fe(Se0.5Te0.5) polycrystalline materials"

[46] N Novosel, S Galic, D Paji ′c,′ Z Skoko, I Lon ˘ carek, M Mustapi ˘ c, K Zadro ′ and E Babic, "Effect of magnetic NiCoB nanoparticles on superconductivity in MgB2 wires" **26** (2016).

[47] S X Dou1, S Soltanian1, Y Zhao1, E Getin1, Z Chen1,2, O Shcherbakova1 and J Horvat1. "The effect of nanoscale Fe doping on the superconducting properties of MgB2" **18**,710 (2015).

[48] Wel Gao and John B Vander Sande , "Textured BSCCO/Ag superconducting microcomposites with improved critical currenl aensiry mrougn mecnanicai deformation"**5**,316 (1992).

[49] "Chakrapani V Varanasi, P N Barnes, J Burke, L Brunke, I Maartense, T J Haugan , E A Stinzianni, K A Dunn and P Haldar"**19**,137(2006).

[50] Mansoor Farbod ff , Mohammad Rcza Batvandi, "Doping effect of Ag nanoparticles on critical current of YBa2Cu3O7d bulk superconductor" **471**,112-117 (2011).

[51] A. N. Jannah, R. Abd-Shukor, and H. Abdullah, "Effect of Co3O4 Nanoparticles Addition on (Bi,Pb)-2223 Superconductor" **7**,3 (2013).

[52] M. A. Suazlinaa* , S. Y. S. Yusaineea , H. Azhanb , R. Abd-Shukorc , R. M. Mustaqiind, "The Effects of Nanoparticle Addition in Bi-2212 Superconductors" (2014).

[53] Xueguang Dong·Pengfei An·Jing Zhang· Hongguang Zbang·Yongtao Li·Hao Liu· Xiaopeng Ge·Qi Li, "Superconductivity Enhancement in Fe3O4 Doped YBa2Cu3O7−δ" **27**,693-694 (2014).

[54] Amir Zelati·Ahmad Amirabadizadeh· Ahmad Kompany·Hadi Salamati·Jeff Sonier. "Effect of Eu2O3 Nanoparticles Addition on Structural and Superconducting Properties of BSCCO" (2014).

[55] TETSUO OKAl, YOSHITAKA ITOH1, YOUSUKE YANAGI1, HIDEHIKO TANAKA2, SHINICHI TAKASHIMA2, and UICHIRO MIZUTANI, "Mechanical and Magnetic Properties of Zr-YBCO Superconducting Composites"

[56] http://www.doitpoms.ac.uk/tlplib/crystallography3/images/lattice_parameters.gif.

[57] V. V. Krishnaji, and S. Kalyane, "Dielectric Property Study of Polyaniline PbTiO3 composites" Glob. Res. Analys. **2**, 225 (2013).

[58] R. K. Sharma, B. Tiwari, and J. S. Tomar, "Study of Thermal Stability of Metal Carbon Nanotubes by SEM, XRD & TGA" Int. j. innov. res. sci. eng. technol. **3**, 9081 (2014).

[59] http://www.doitpoms.ac.uk/tlplib/xray-diffraction/images/labelled.jpg.

[60] http://www.analyticalchemistrygsu.com/2013/03/braggs-law-with-applications-and.html.

[61] S. Singh, H. Kaur, D. Pathak, and R.K Bedi, "Zinc oxide nanostructures as transparent window layer for photovoltaic application" Dig. J. Nanomater. Bios. **6**, 689 (2011).

[62] M. Fakhar-e-Alam, M. A. Asghar, U. Nazar, S. Javed, Z. Iqbal, M. Atif, S. M. Ali, and W. A. Farooq, "Characterization of zinc oxide (ZnO) thin film coated by thermal evaporation technique" J. Optoelectron. Biomed. Mater. **6**, 35 (2014).

[63] K. T. Lau, M. Lu, and L. Hui, "Coiled carbon nanotubes: Synthesis and their potential applications in advanced composite structures" Composites Part B **37**, 437 (2006).

[64] G. Gilli, "Fundamentals of Crystallography" Oxford university press, U.K. (2002).

[65] B.E. Warren, "X-ray Diffraction" Courier corporation, U.S.A. (1969).

[66] C. Kittel "Introduction to solid state physics" 7th ed. Wiley, India (1995)

[67] H. P. Klug, and L. E. Alexander, "X-Ray diffraction procedures: for polycrystalline and amorphous materials" 2nd ed. Wiley-interscience, New York (1974).

[68] B.Cheney, "Introduction to scanning electron microscopy" San Jose State University press (1995).

[69] Syed Alamdar Hussain Shah, "Vibrating Sample Magnetometery: Analysis and Construction" Department of Physics, Syed Babar Ali School of Science and Engineering, LUMS Friday, December, **13**, (2013).

[70] R. Manigandan, K. Giribabu , R. Suresh , L. Vijayalakshmi , A. Stephen and V. Narayanan, "Cobalt Oxide Nanoparticles: Characterization and its Electro catalytic Activity towards Nitrobenzene", Chem. Sci. Trans. 2(S1) (2013) S47

[71]] L. Ali, M. Mumtaz, I. Ali, M. Waqee-ur-Rehman, and A. Jabbar, "Metallic Cu Nanoparticles Added to $Cu_{0.5}Tl_{0.5}Ba_2Ca_2Cu_3O_{10-\delta}$ Superconductor", J. Supercond. Nov. Magn. (2017). https://doi.org/10.1007/s10948-017-4229-8

[72] R. S. Meena, Anand Pal, Shiva Kumar, K.V.R. Rao and V.P.S. Awana, "Magneto-transport and Magnetic Susceptibility of $SmFeAsO_{1-x}F_x$ (x = 0.0 and 0.20)" J. Supercond. Nov. Magn. **26**, 2383 (2013).

[73] G. Kırat a , O. Kızılaslan b , M.A. Aksan, "Effect of the Er-substitution on critical current density in glass-ceramic Bi2Sr2Ca2(Cu3-xErx)O10+δ superconducting system" **42**,15072 (2016).